Composition of Phenocrysts in Lamproites of Gaussberg Volcano, East Antarctica

N. A. Migdisova[a, *], **N. M. Sushchevskaya**[a, **], **M. V. Portnyagin**[b],
T. A. Shishkina[a], **D. V. Kuzmin**[c], **and V. G. Batanova**[d]

[a] *Vernadsky Institute of Geochemistry and Analytical Chemistry, Russian Academy of Sciences, Moscow, 119991 Russia*
[b] *GEOMAR Helmholtz Centre for Ocean Research Kiel, Kiel, 24148 Germany*
[c] *V.S. Sobolev Institute of Geology and Mineralogy of the Siberian Branch of the Russian Academy of Sciences (IGM SB RAS), Novosibirsk, 630090 Russia*
[d] *Univ. Grenoble Alpes, Univ. Savoie Mont Blanc, CNRS, IRD, Univ. Gustave Eiffel, ISTerre, Grenoble, 38000 France*
*e-mail: nat-mig@yandex.ru
**e-mail: nadsus@gmail.com

Abstract—This paper presents numerous new data on the geochemical composition of olivine, clinopyroxene, and leucite phenocrysts, as well as spinel inclusions in olivine and quench glass from lamproites of Gaussberg volcano (East Antarctica). Most of the olivine phenocrysts in the Gaussberg lamproites are high Mg varieties (Fo_{89-91}) with elevated Ni contents (up to 4900 ppm) and high Ni/Co ratios. According to data of about 320 clinopyroxene analyses, two groups of diopsidic phenocrysts have been established. Group I consists mainly of high-Mg varieties (Mg# >80), while group II clinopyroxenes are less magnesian (Mg# 52–80). The main difference between the clinopyroxenes of the two groups is the elevated contents of Al_2O_3, FeO and reduced TiO_2, Cr_2O_3, and NiO in the compositions of group II compared to group I, as well as different contents of trace elements, which may reflect their crystallization from different types of primary melts. According to the study of ~550 grains of leucite phenocrysts in the Gaussberg lamproites, it was shown that they correspond to the ideal stoichiometry of leucite $K[AlSi_2O_6]$ and are enriched in Na_2O (0.05–0.35 wt %), but depleted in K_2O (19.9–20.9 wt %) compared to leucites from lamproites of other provinces. The BaO content reaches 0.3 wt %, SrO –0.04 wt %. The iron content in most leucite phenocrysts varies within 0.7–1.2 wt % Fe_2O_3, but some grains have the low Fe_2O_3 contents (<0.5 wt %). In leucite microlites of the groundmass and rims of phenocrysts, the Fe_2O_3 content can reach 2.4 wt %, which may indicate more oxidized conditions at lava eruption. Based on the study of natural samples, existing experimental data and numerical models, the order and conditions of crystallization of the Gaussberg lamproites were obtained. Crystallization proceeded in the following order: chromian spinel → chromian spinel + olivine → olivine + leucite (± chromian spinel) → olivine + leucite + clinopyroxene (± chromian spinel). The near-liquidus assemblage represented by high-Mg olivine phenocrysts with inclusions of Cr-spinel was formed in the temperature range from 1180 to 1250°C. Further crystallization of the melt with the formation of an association of olivine+leucite+clinopyroxene phenocrysts could occur at pressures below 2 GPa and temperatures of 1070–1180°C, corresponding to the presence of water in the magmatic system. Estimates of the redox conditions of crystallization of lamproites obtained using different oxybarometers vary in a wide range from QFM-0.5 to QFM+2.3. The elevated Ni contents in liquidus olivines of Gaussberg indicate the high nickel contents in the source. It is shown that the formation of ultra-alkaline magmas in the Gaussberg volcano area is likely related to melting of the continental lithosphere, which was heterogeneous and included both the peridotite mantle and hydrous pyroxenite fragments.

Keywords: olivine, clinopyroxene, leucite, lamproites, ultra-alkaline rocks, Gaussberg, Antarctica, pyroxenite, peridotite, redox conditions, crystallization temperature, mantle source

DOI: 10.1134/S0016702923090082

INTRODUCTION

Lamproites are scarce ultra-alkaline magnesian rocks having low CaO, Al_2O_3, and Na_2O contents, elevated Mg#, and high K_2O/Al_2O_3 and K_2O/Na_2O ratios (Foley et al., 1987; Jaques et al., 1984). The manifestations of lamproite magmatism of different age were found in many regions of the Earth. These are, for instance, Leucite Hills (Wyoming, USA), West Kimberly (Australia), ultra-potassic volcanics of the Mediterranean volcanic belt, the western part of the East African rift, and volcanic fields in Northeast China (Foley et al., 1987; Gupta, 2015). The reasons for the

special interest to these rocks are related to the discovery of diamonds in lamproites of West Australia (Sobolev, 1976; Atkinson et al., 1984; Jaques et al., 1984).

In spite of the comprehensive study of the problem of lamproite formation during the last decades, their origin remains controversial (Gupta, 2015). The formation of lamproites is thought to be related to the low-degree melting of enriched mantle, which explains their unusual enrichment in incompatible trace elements compared to other ultramafic mantle rocks (Sun et al., 2014; Murphy et al., 2002; Foley and Jenner, 2004). However, many questions remain debatable, in particular, the depth of enriched mantle source: whether it is located in subcontinental lithosphere mantle (SCLM) (Avanzinelli et al., 2008; Chen et al., 2007; Chu et al., 2013; Davies et al., 2006; Prelevic et al., 2008; Zhang et al., 1995; Zou et al., 2003), in asthenosphere (Choi et al., 2006), or in the transitional mantle zone (Kiritani et al., 2013; Murphy et al., 2002). It is believed that the origin of metasomatizing fluids and/or melts that significantly enriched their source is related to the involvement of deep-seated asthenospheric mantle (McKenzie, 1989; Zhang et al., 2000), subduction zone (Elburg, Foden, 1999), delaminated subcontinental lithospheric mantle (Choi et al., 2006), transition mantle zone (Kiritani et al., 2013; Murphy et al., 2002), or delaminated lower continental crust (Chu et al., 2013).

Experimental melting of ultramafic rocks enriched in hydrous minerals (phlogopite or K-richterite) with accessory ilmenite, rutile, and apatite yielded melts of lamproite composition at 1.5 and 5 GPa (Foley et al., 2022). These experiments showed that the important components of mantle source of most magmatic rocks were hydrous pyroxenites with diverse accessory mineral phases (Foley et al., 2022). Deep-seated high-K melts formed during their melting could change their composition through the interaction with host mantle rocks of peridotite composition. This could lead to the formation of basaltic volcanic rocks with peridotite signatures due to the dilution of initial contribution of hydrous pyroxenites, even though the temperature in the source region remains much lower than the melting point of peridotite (Foley et al., 2022). The possible modification of magma composition during ascent from a mantle source to the surface complicates the unambiguous deciphering the origin of primary lamproite magmas. In addition, it is necessary to take into account the heterogeneity of cratonic mantle both on regional and local scales, for instance, the possible presence of domains intersected by "veins" of melts of different melting stages. Such local heterogeneity was revealed for a source of alkaline magmas from the Aldan shield (Chayka et al., 2020). For this reason, the question of composition of source and primary ultra-alkaline magmas should be individually solved for each definite case with allowance for the evolution of the given continental area. Generally, the origin of lamproites is thought to be related to melting of

reworked ancient sublithospheric mantle beneath the Proterozoic−Paleozoic cratons in the presence of essentially aqueous fluid at low CO_2 activity (Edgar and Mitchell, 1997; Foley and Jenner, 2004; Sushchevskaya et al., 2014).

Lamproites of Gaussberg volcano (East Antarctica) is the Earth's only occurrence of this rock type in form of pillow lavas, which erupted under subice conditions and represent the Earth's youngest lamproites (56000 ± 5000 years, Tingey et al., 1983) (Fig. 1). At first, these rocks were termed leucitites owing to the presence of leucite phenocrysts, but then were renamed lamproites or leucite lamproites according to the IUGS classification (International Union of Geological Sciences) (Smellie and Collerson, 2020). The uniqueness of the Gaussberg ultra-alkaline rocks significantly enriched in K_2O (up to 11−12 wt %) makes them important petrological object for study, especially with allowance for the influence of excess alkalis on the temperature of generation and subsequent crystallization of mafic magmas. Based on classification (Foley et al., 1987), the lamproites of Gaussberg, as those of West Kimberly, are ascribed to the group of melts having the low CaO, $A1_2O_3$, and Na_2O contents, high Mg#, and high $K_2O/A1_2O_3$ ratio. Recent Mg and Zn isotopic data showed that a source of the Gaussberg lamproites could be either subcontinental mantle metasomatized by carbonate melts or residue of subducted carbonate-bearing sediments after melting in the mantle transitional zone (Liu et al., 2022).

This work is dedicated to the detailed study of phenocryst assemblage in the lamproites of Mt. Gaussberg, which were obtained during 2nd Soviet Antarctic Expedition in 1956−1958 (Vyalov and Sobolev, 1959). For this purpose, we analyzed the major and trace element compositions of the main mineral phases (olivine, clinopyroxene, leucite, and spinel), as well as quench glass, using modern analytical methods, which significantly expanded the results of previous mineralogical studies of the Gaussberg lavas (Foley, 1985; Foley and Jenner, 2004; Salvioli-Mariani et al., 2004). One of the main tasks of this study was to estimate physicochemical conditions and order of the crystallization of high-K Gaussberg magmas, as well as to determine the contribution of pyroxenites in a mantle source of lamproite melts based on obtained analytical data.

GEOLOGICAL POSITION OF GAUSSBERG VOLCANO

Mount Gaussberg (Fig. 1) is located on the eastern coast of the Princess Elizabeth Land (Kaiser Wilhelm II Land) (coordinates of 66°47′ S, 89°18′ E). It was produced by subice volcanic eruption and represents an isolated cone approximately 370 m high (Golynsky and Golynsky, 2007). The surface of the volcano is covered by pillow lavas in which separate pillows reach 0.5−2 m across and frequently have well
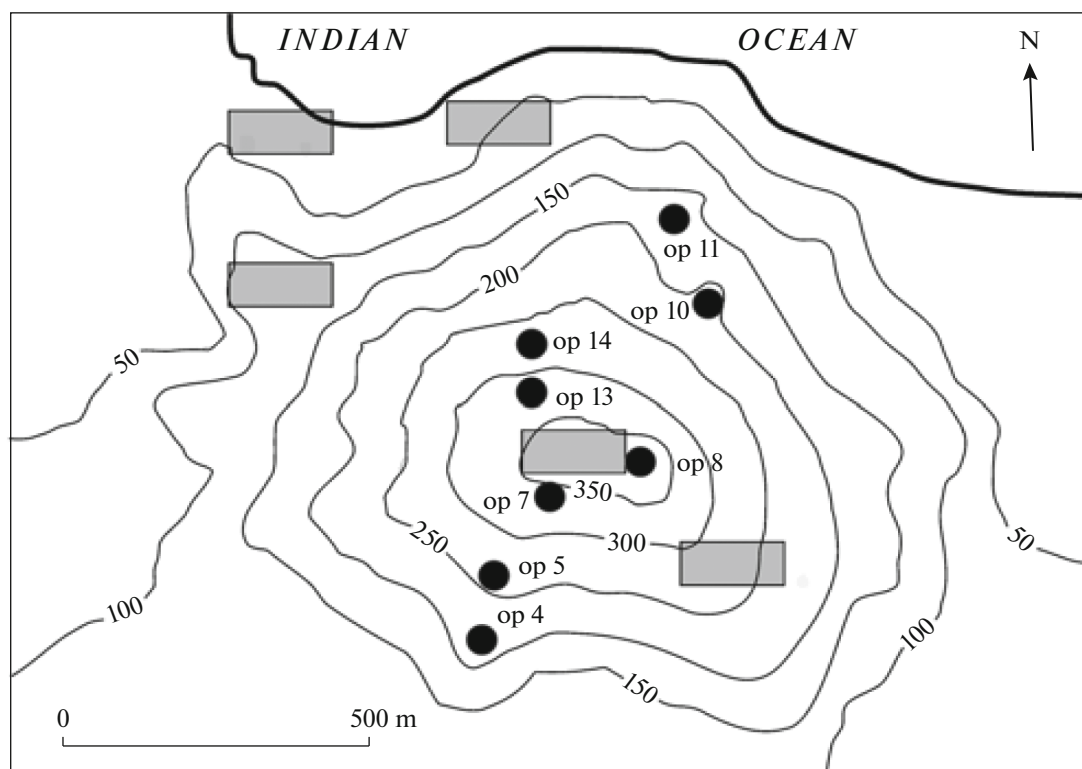
Fig. 1. Position of sampling stations in the topographic scheme of Mt. Gaussberg (Sushchevskaya et al., 2014). Observation points (op) 1−3, 15−24 are located near the foot of the southern slope of the volcano and are not seen in the presented sampling scheme. The distribution of the studied samples over observation points (op): 1—sample 458 (OG2); 2—samples 459 (OG3), 460 (OG4), 461 (OG5); 4—samples 462 (OG6), 464 (OG8), 5—sample 465 (OG9); 7—samples 468 (G12), 469 (G13), 470 (G14), 482 (G26); 8—sample 471 (G15); 10—samples 475 (G19), 476 (G20); 11—sample 477 (G21); 13—sample 479 (G23); 14—sample 480 (G24). Gray boxes show sampling stations in the Australian expeditions (Sheraton and Cundari, 1980).

preserved black glassy quench crust 3−5 cm thick, as well as lava fragments or tuff breccia. The volcano was found in 1902 during German Antarctic Expedition of the Gauss vessel which gave name to the volcano (Von Drygalski, 1989). Later, this area was studied during the First and Second Soviet Antarctic Expeditions in 1955−1958 (Vyalov and Sobolev, 1959; Glebovsky, 1959), as well as during the Australian Antarctic Expeditions in 1977, 1987, and 1997 (Sheraton and Cundari, 1980; Golynsky and Golynsky, 2007).

According to data of echolocation and RADARSAT system, Gaussberg volcano sits on the Gaussberg Ridge extending for over 500 km (Golynsky and Golynsky, 2007). Submarine part of the ridge extends up to the volcanic structures of Kerguelen Island, while terrestrial part is exposed on the Antarctic coast, continuing up to Mt. Brown (Leitchenkov and Guseva, 2006). The inferred Gaussberg rift, on which volcanic edifices sit, was likely initiated simultaneously with the Lambert Graben and ascribed to the Lambert rift system (Leitchenkov and Guseva, 2006; Golynsky and Golynsky, 2007).

According to K-Ar dates, the Gaussberg lamproites were formed in the Late Pleistocene (56000 ± 5000 years, Tingey et al., 1983).

Previous studies of the composition of the Gaussberg lavas showed that pillow lava samples taken in different points of the volcano and ascribed to different lava flows have close chemical composition, which varies in narrow ranges and represents high-K (11−12 wt % K_2O), rocks that are extremely enriched in trace elements and correspond to lamproites (Sheraton and Cundari, 1980; Sheraton, 1981; Murphy et al., 2002; Sushchevskaya et al., 2014).

The Sr and Nd isotope composition of the lamproite lavas of Gaussberg indicates an extremely high enrichment of a mantle source (Williams et al., 1992; Nelson et al., 1986; Murphy et al., 2002; Sushchevskaya et al., 2014). The initial Nd isotope composition varies from −13 to −15 (ϵNd), while $^{87}Sr/^{86}Sr$, from 0.7092 to 0.7109. According to (Nelson et al., 1986), the enrichment age for a source of the Gaussberg lamproite melts is estimated at 1.4−1.8 Ga using U−Th−Pb isotopic system. Nelson et al. (1986) believe that the lamproites were derived from very old mantle source, which had high U/Pb ratio at the early evolution stage, and younger source with lowered U/Pb, which are typical of tholeiitic oceanic melts (MORB, mid ocean ridge basalts) at the late stage. Based on the Pb isotope variations, the mantle source

of the lamproites of Gaussberg volcano involved ancient material that was depleted in lithophile elements, i.e., uranium (low U/Pb), which led to the low $^{206}Pb/^{204}Pb$ ratios, but was enriched in ^{207}Pb and ^{208}Pb (Sushchevskaya et al., 2014). This could be caused by the input of "ancient" uranium (in which the fraction of ^{235}U was much higher than in the modern uranium) and thorium.

SAMPLES AND METHODS

In this work, we studied the compositions of mineral and glassy phases in 16 lamproite samples from Mt. Gaussberg, the chemical and isotopic composition of which was previously described by Sushchevskaya et al. (2014). The majority of the studied samples have close petrographic features, mineralogical and chemical composition. Due to the compositional homogeneity, the Gaussberg lavas were not divided into groups but were considered as a whole, which was also made in previous studies (Sheraton and Cundari, 1980; Murphy et al., 2002).

Rock samples represented fragments of unaltered pillow lavas 1−2 kg in weight with glassy, aphanitic, or porphyritic texture. The lavas are porous, and pore sizes increase from rim to core of the pillows. The typical Gaussberg lamproites have the following modal composition: phenocrysts of olivine (10%), clinopyroxene (5%), leucite (20−40%), as well as glassy or aphanitic groundmass (30−60%) (Figs. 2a, 2b, 3, 4). The phenocrysts are usually 0.3−2 mm in size and occur as separate euhedral and subhedral grains, and as glomeroporphyric intergrowths (Figs. 2c, 2d). The olivine phenocrysts contain inclusions of chromian spinel (Fig. 2f). The leucite and olivine contain glassy melt inclusions (Figs. 2b, 2d). The groundmass is made up of quench glass and microlites of leucite, clinopyroxene, phlogopite, and apatite (Figs. 2a, 2b). Some samples contain large grains of leucite (up to 2 mm) of irregular shape, with traces of secondary alterations and frequently forming intergrowths with green clinopyroxene (Fig. 2f, Suppl. 1).

For analytical studies, phenocryst grains and fragments of quench glass collected from ground samples of the Gaussberg lamproites (fraction of 0.25−1 mm) were mounted into pellets with epoxy resin 2.5 cm across. Over 390 olivine phenocrysts (Suppl. 2, Table S2), 320 clinopyroxene grains (Suppl. 2, Table S3a, S3b, S3c), 550 leucite grains (Suppl. 2, Table S4) and quench glass (~ 30 analyses) were analyzed in studied samples at the Max Plank Institute for Chemistry (Mainz, Germany or MPI-Mainz) on an X-ray Jeol JXA 8200 Superprobe microprobe. The compositions of olivines were analyzed at an accelerating voltage of 20 kV and probe current of 300 nA using procedure developed by (Sobolev et al., 2007; Batanova et al., 2011). The 2σ error was 20−30 ppm for the measurements of Ni, Ca, Mn, Al, Ti, Cr, and Co contents and 0.02 mol %

for forsterite olivine component. Spinel composition was measured at 20 kV and probe current of 80 nA. The synthetic standard P&H Developments Ltd., Calibration Standards for Electron Probe Microanalysis, Standard Block GEO for all elements and rhodonite for Mg were used for calibration. The compositions of clinopyroxene and leucite were determined using conventional technique at an accelerating voltage of 20 kV and beam current of 20 nA. International natural minerals from the Smithsonian collection, Washington, USA (Jarosewich et al., 1980) were used as standards. Standard ZAF correction was applied to analyses of all minerals.

Some analyses of olivine, as well as spinel inclusions (15 analyses) in olivine phenocrysts (Suppl. 2, Table S5) were made on a JEOL JXA 8230 microprobe at the ISTerre, University of Grenoble Alpes, using high-precision trace element determination (Batanova et al., 2015). With this technique, olivine, in addition to Mg, Fe, and Si, was analyzed for trace Na, Al, P, Ca, Ti, Ni, Mn Zn, Cr, and Co. The following parameters were applied: accelerating voltage 25 V, a probe current of 900 nA on a Faraday cup. Trace elements were measured on five wavelength dispersion spectrometers, while major elements were measured on an energy dispersive spectrometer. The counting time in one point was 12 min. The San Carlos USNM 111312/44 reference olivine (Jarosewich et al., 1980) was analyzed three times after every 30 points. This allowed the control and correct the instrumental drift. The analytical reproducibility established by repeated measurement of olivine standard as two standard deviations from mean accounts for 4−10 ppm for most trace elements, 15 ppm for Na, and 300 ppm for major elements.

The contents of trace elements in clinopyroxenes and some olivines were determined at the Max Plank Institute for Chemistry (Mainz, Germany) by inductively coupled plasma mass spectrometry LA-ICP-MS on a Thermo Finnigan Element 2 mass spectrometer coupled with a Merchantek 213 nm New Wave UP213 laser ablation microprobe. The diameter of laser beam was 80 µm. A mixture of helium and argon was used as a gas carrier. The background was ablated for 20 s, while sample, for 80−100 s. The reference glasses KL2-G and NIST 612 were used as standards. Calcium contents obtained on microprobe were taken as internal standard for recalculation of intensities for clinopyroxenes. The measurement accuracy for most elements was no less than 4% (Batanova et al., 2015). The contents of trace elements in olivine were also determined by LA-ICP-MS at GEOMAR, Kiel, Germany. Analyses were carried out on an Agilent 7500s mass spectrometer attached to the GeolasPro Cogerent laser ablation system. The beam size was 60 microns. Other conditions of analysis and standardization were similar to those described in (Sobolev et al., 2016).

Quench glasses (Suppl. 2, Table S1) were analyzed on an electron microprobe at the Max Plank Institute
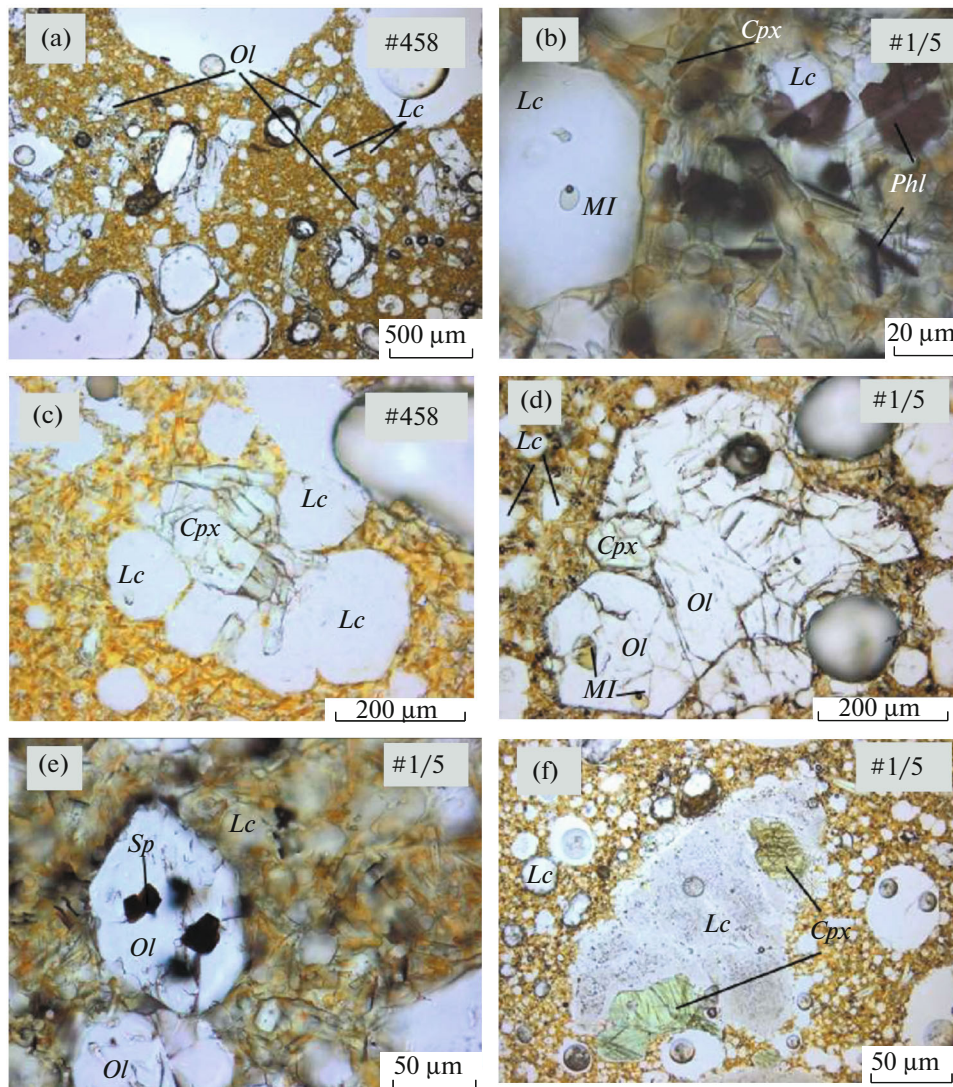
Fig. 2. Mineralogical-petrographic features of the Gaussberg lamproites (samples 458 and 1/5) (microphotographs of thin sections in transmitted light, without analyzer). (a) A general view of the rock (sample #458): phenocrysts and microphenocrysts of olivine and leucite, as well as pores in finely crystallized groundmass consisting of microlites of leucite, clinopyroxene, with possible presence of apatite. (b) Groundmass of the rock (sample #1/5): microlites of leucite, clinopyroxene, and phlogopite. Leucite microphenocryst contains melt inclusions. (c–d) Intergrowths of leucite, olivine, and clinopyroxene phenocrysts (samples 458 and #1/5). (e) Olivine microphenocryst with chromian spinel inclusions; (f) intergrowth of large leucite phenocryst with traces of secondary alteration and green clinopyroxene phenocryst (sample #1/5). Abbreviations: *Ol*—olivine, *Lc*—leucite, *CPx*—clinopyroxene, *Sp*—chromian spinel, *MI*—melt (glassy) inclusion, *Phl*—phlogopite. Additional microphotographs of the Gaussberg lamproites are listed in Suppl. 1.

for Chemistry, Mainz, Germany on an X-ray analyzer equipped with a Jeol JXA 8200 Superprobe microprobe, as well as with LA-ICP-MS at the GEOMAR, Kiel, Germany, using technique described in (Sobolev et al., 2016).

COMPOSITIONS OF QUENCH GLASSES AND PHENOCRYSTS

Quench Glass

The Gaussberg lamproites are unique in the presence of fresh quench glasses formed by subice eruption. The compositions of quench glasses determined in this work and the bulk compositions of the studied samples published in (Sushchevskaya et al., 2014) are given in Table S1 (Suppl. 2) and in Figs. 5, 6, 7. As was shown above, the bulk compositions of the Gaussberg lamproites vary within narrow ranges (51.5–53.5 wt % SiO_2, 7.5–8.3 wt % MgO) (Fig. 5). The homogeneity of bulk compositions of the Gaussberg lavas, unlike glasses of Gausberg, rather reflects insignificant contribution of crystallization and precipitation of phenocrysts from melt at the early stages of magma ascent. This led to the absence of differentiation trend, unlike other lamproite series, for instance, West Kimberly (West Australia) and Leucite Hills
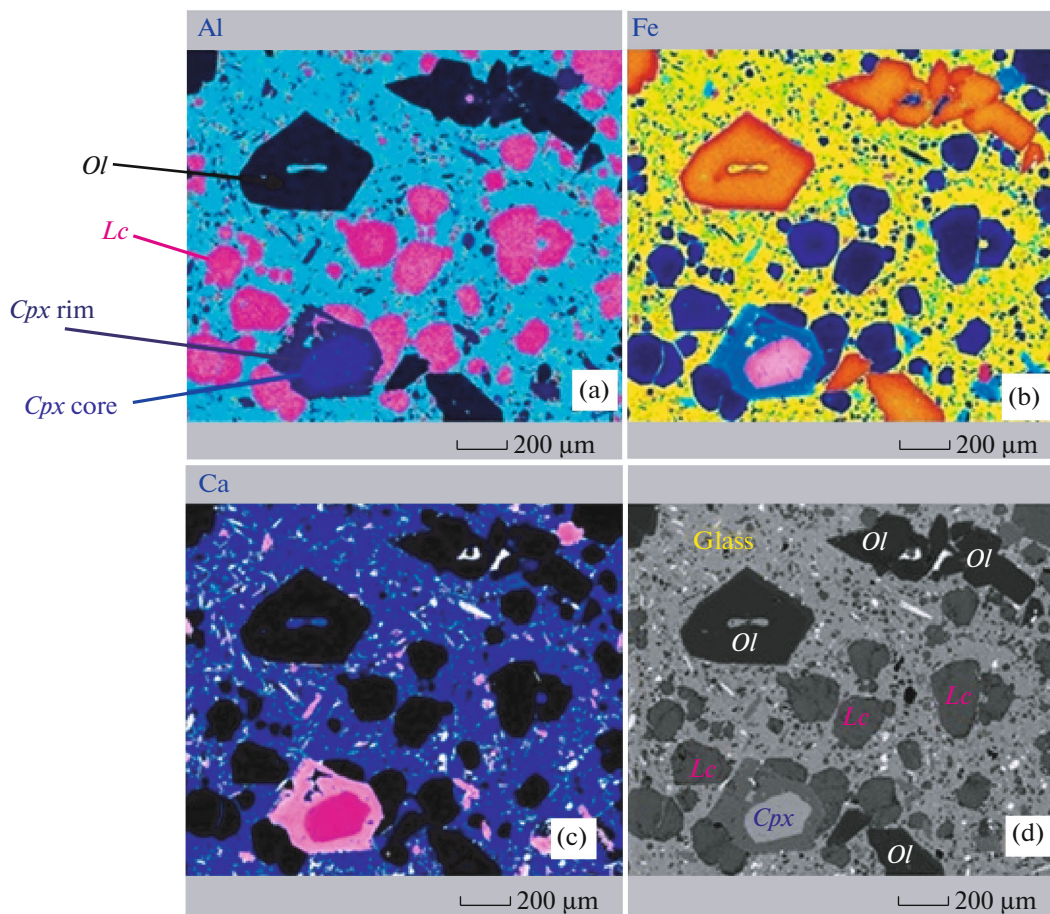
Fig. 3. Images of area of sample #475, obtained using electron microprobe. (a), (b), (c) Al, Fe, and Ca distribution maps (elements concentrations decrease from red to dark-blue), (e) Back-scattered electron (BSE) image. Shown are phenocrysts: olivine (*Ol*), clinopyroxene (*Cpx*), and leucite (*Lc*) in a partly crystallized groundmass consisting of quench glass (Glass) with microlites.

(Wyoming, USA) (Murphy et al., 2002). Thereby, the compositions of quench glasses in the Gaussberg lavas define a differentiation trend from relatively primitive compositions (51.5 wt % SiO_2, 6.7 wt % MgO) to more evolved rocks (56.8 wt % SiO_2, 1.6 wt % MgO) (Fig. 5).

The glasses of the Gaussberg lamproites have sufficiently high contents of volatile components (Fig. 6). A systematic decrease of phosphorus concentration (from 1.9 to 0.7 wt % P_2O_5) with differentiation of residual melt could be explained by apatite crystallization. The contents of sulfur and chlorine, in contrast, increase (from 0.02 to 1.0 wt % S and from 0.13 to 0.27 wt % Cl) with melt evolution. Such trends could indicate the accumulation of these volatile components in the melt in intermediate chambers and subsequent rapid quenching at magma ejection.

Based on the contents of trace lithophile elements, the compositions of quench glasses inherit characteristic features of the bulk compositions of Gaussberg lamproites. The primitive mantle-normalized distribution patterns of lithophile elements show Ba, La, Pb, Sr, Zr, and Hf maxima and U, Nb, Ta, and Sm minima (Fig. 7).

Olivine

Olivine phenocrysts in the Gaussberg lamproites are usually colorless, but sometimes have pale yellow tint. Some olivine phenocrysts contain glassy melt inclusions or inclusions of chromian spinel (Fig. 2f).

The microscopic and microprobe studies revealed that olivine has no major and trace-element zoning (except for phosphorus), but its rim differs in composition from the core (Fig. 3). Figure 8 shows the element distribution maps of typical olivine grain in the Gaussberg lamproites. It is seen that the grain is compositionally homogenous, and only its rim is enriched in Ca and Fe, which can indicate its crystallization from more evolved melt or a change of composition of marginal part of olivine through the re-equilibration with residual melt. However, in terms of phosphorus content, the grain shows multiple oscillatory zoning, which may indicate the different rate of the grain growth at different crystallization stages (P-rich zones are formed at rapid crystal growth) (Milman-Barris et al., 2008). The absence of zoning for other trivalent cations in olivine grain (Cr and Al) may indicate a relatively long residence time of phenocrysts in a hot
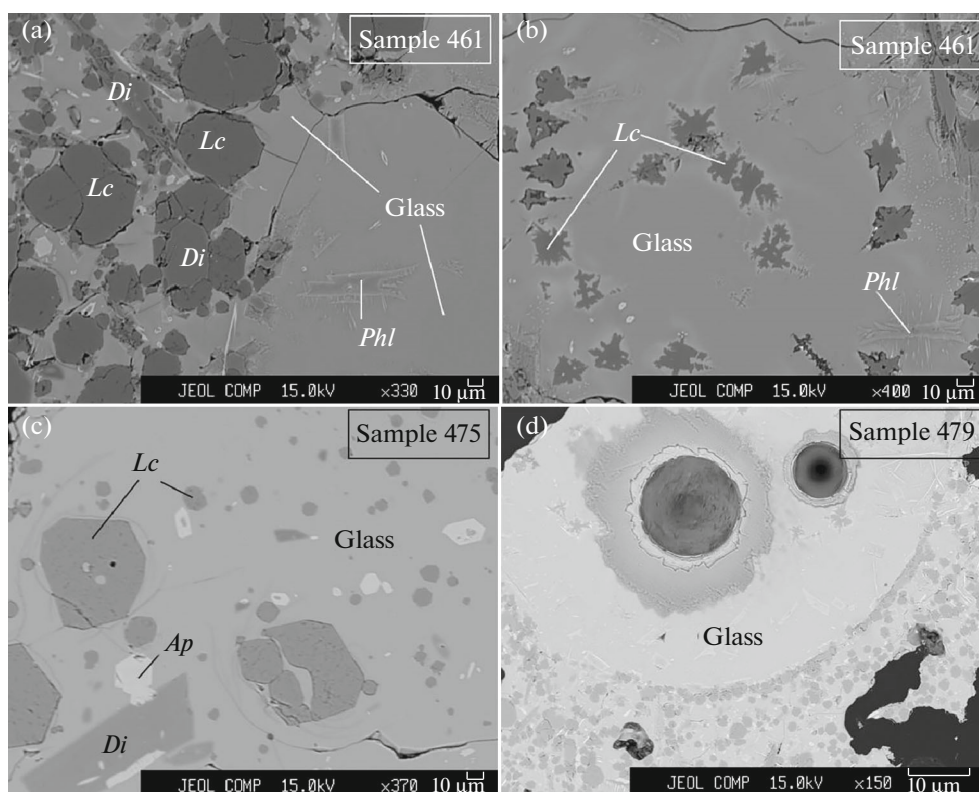
Fig. 4. BSE images of groundmass in the studied lamproite samples of Gaussberg volcano. (a–b) Sample #461: microlites of leucite (*Lc*), diopside (*Di*), and phlogopite (*Phl*) are embedded in a glassy mass (Glass). (c) Sample #475: microlites of leucite (*Lc*), diopside (*Di*), and apatite (*Ap*) are distributed in a glassy matrix; d) sample #479: area of sample at the contact of quench glass (Glass) and aphanitic groundmass. Round pit is the crater remained after glass analysis with LA-ICP-MS.

magma, which caused the re-equilibration of concentrations of these elements within a single grain, as for divalent cations (Milman-Barris et al., 2008). Thereby, phosphorus zoning in olivine has been preserved due to the extremely low diffusion rates for this element in olivine (Milman-Barris et al., 2008).

Among ~ 400 analyses of selected olivine phenocrysts, high-Mg olivines Fo 89–91 account for practically 95% (Table S2, Suppl. 2). At the same time, scarce phenocrysts contain higher Fe olivines (up to Fo_{84}), which indicates the melt fractionation.

Variations of trace element contents in the Gaussberg olivines demonstrate systematic changes corresponding to the melt evolution during crystallization. There are accumulation trends of Mn from 1100 to 3000 ppm, Co from 110 to 180 ppm, whereas Ni and Co contents decrease from 4800 to 1800 ppm and from 500 to 100 ppm, respectively (Fig. 9). To reveal the compositional features of olivine phenocrysts from the Gaussberg lamproites, they were compared with literature data on similar geological objects. Figure 9 reports compositions of olivine from picritic lavas and lherzolite inclusions in lavas of the Jetty alkaline province, which is located in East Antarctica and was formed in relation with the Kerguelen plume activity at ~ 117–110 Ma (Sushchevskaya et al., 2018). The

high-Mg Jetty ultra-alkaline association shown for comparison contains 20–25% olivine, ~ 1–2% pyroxene, and ~ 5% Ti-magnetite with varying admixture of phlogopite and carbonates, which was formed through melting of metasomatized continental mantle at T ~ 1270°C and at depth around 130–140 km (Sushchevskaya et al., 2017). Lherzolite mantle inclusions in the Jetty alkaline lavas reflect the composition of continental mantle beneath East Antarctica (Sushchevskaya et al., 2017). Figure 9 also demonstrates variations of olivine from mafic tholeiitic magmas of South Atlantic (PetDB, shown by field) and flood basalts of the Queen Maud Land (Antarctica) (Grantham et al., 1996). It should be noted that the Gaussberg olivines differ from other olivines in the elevated Ni contents and high Ni/Co ratios. Compared to the olivines from the Jetty alkaline province, they have the higher Ni and Ca contents and lowered Al concentrations.

Thereby, single high-Mg olivines differ in the lowered contents of calcium (< 1000 ppm Ca) and aluminum (< 20 ppm Al), which are close to those of olivines found in mantle nodules from the Jetty oasis (Fig. 9). The Ca contents in most magnesian Gaussberg olivines are higher (~ 1000 ppm) compared to the Jetty olivines (500 ppm), but lower than Ca contents in olivines from
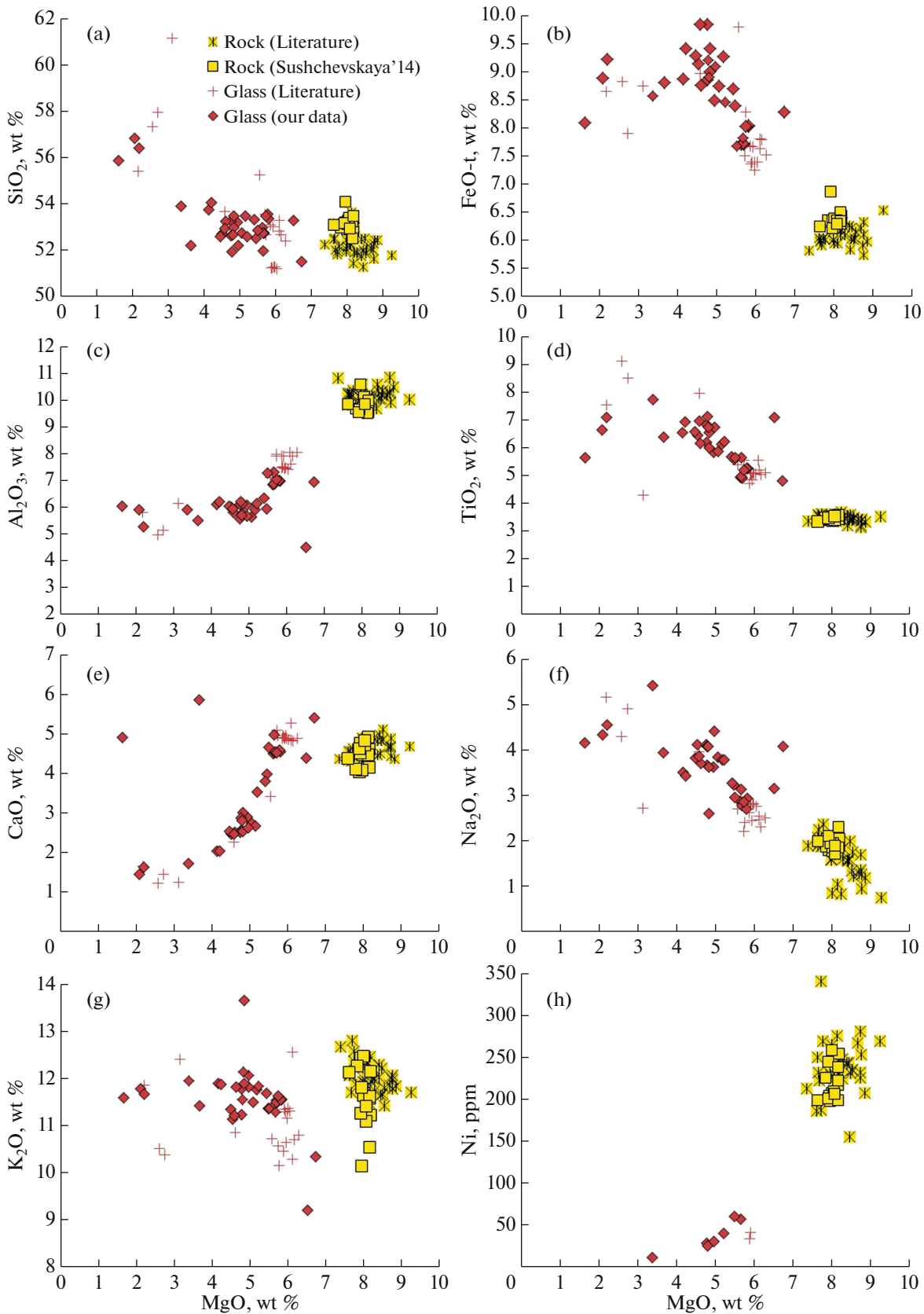
Fig. 5. Contents of major elements in quench glasses and rocks of Gaussberg volcano. Glasses are data of this work. Rocks are taken from Sushchevskaya et al. (2014). Also are given the compositions of quench glasses and rocks after literature data (Sheraton and Cundari, 1980; Sheraton, 1985; Murphy et al., 2002; Foley and Jenner, 2004; Salvioli-Mariani et al., 2004).
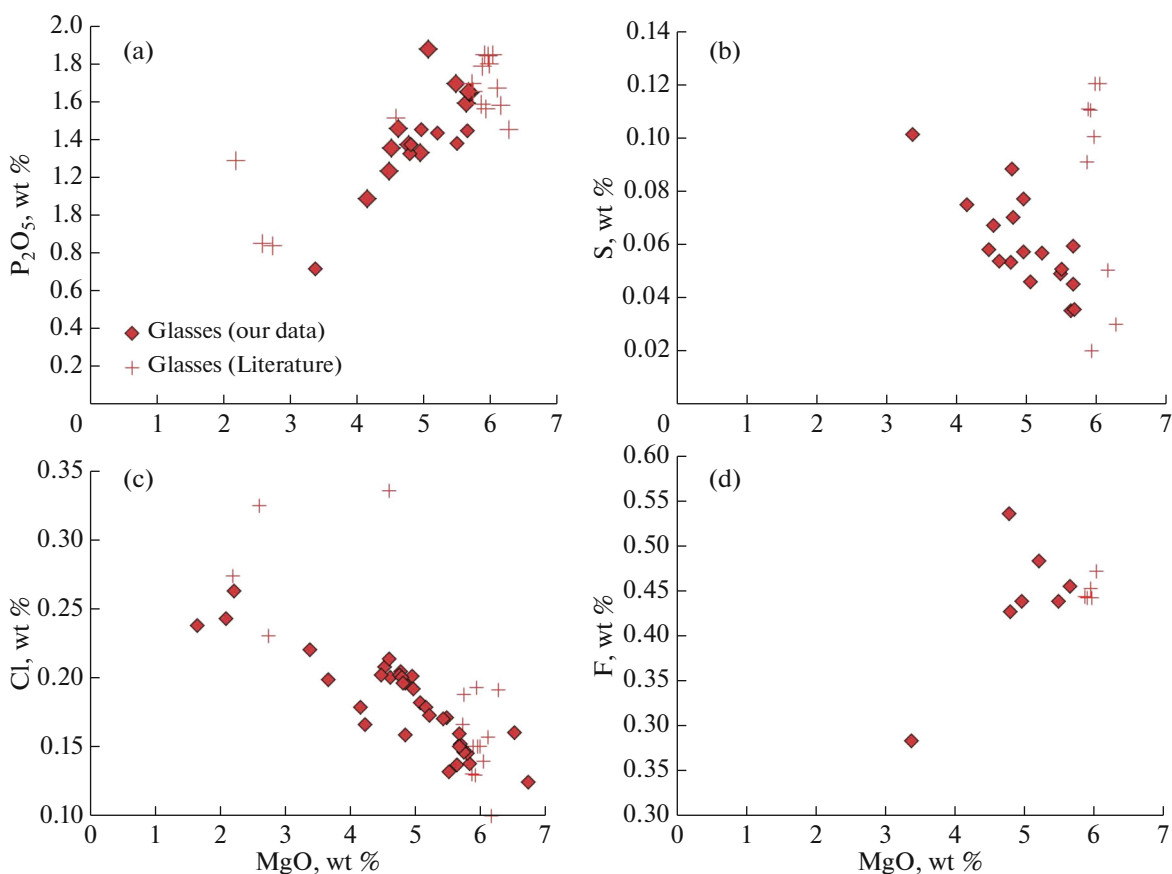
Fig. 6. Contents of volatiles in quench glasses of Gaussberg volcano depending on the MgO contents (wt %) using our and literature data (Sheraton and Cundari, 1980; Foley and Jenner, 2004; Salvioli-Mariani et al., 2004).

the Antarctic flood-basalt province (1800 ppm). The values of Mn content and Mn/Fe ratio in the Gaussberg olivines are higher than in olivines from alkaline picrites and lherzolite nodules from the Jetty oasis, but are lower than those from olivines of the Queen Maud Land. The NiO/CoO ratio in the magnesian olivines of Gaussberg (~40) is much higher than that of the Jetty alkaline picrites (~20). In olivine Fo_{89} and lower, this parameter sharply decreases, approaching 15, which is close to the values of these ratios in the Jetty olivines (Fig. 9).

Figure 10 shows variations of Li, Ti, Zn, and V/Sc in the studied samples. The Li content (~5 ppm) in olivines from the Gaussberg lamproites are lower Li than those of the Mediterranean olivines, but are higher compared to olivines from ocean-island basalts (0–3 ppm) (Foley et al., 2013). According to (Foley et al., 2013), the elevated Li contents (from 10 to 45 ppm) in the alkaline basalts of the Mediterranean volcanic belt could be related to the admixture of continental sediments in a source. Thereby, the Li content in olivines from peridotites is no more than 1–5 ppm, usually accounting for 2 ppm (Foley et al., 2013).

The Zn content in olivines of the Gaussberg lamproites varies within a narrow range from 130 to 160 ppm,

whereas olivines from the Mediterranean lamproites contain from 100 to 300 ppm Zn. The Ti content in the Gaussberg olivines accounts for from 80 to 120 ppm, which corresponds to the compositional range of Mediterranean olivines (from 40 to 120 ppm), but is lower than in olivines from common continental or within-plate basalts (Prelevic and Foley, 2007; Prelevic et al., 2013). The values of V/Sc ratio in the Gaussberg olivines account for 0.8–0.9, which is lower than the V/Sc ratio (from 1 to 5) determined in olivines from the Mediterranean alkaline rocks.

Clinopyroxene

In this work, we studied ~ 300 separate clinopyroxene phenocrysts in samples from all sampling stations. Clinopyroxene phenocrysts in the Gaussberg rocks are represented by sufficiently large greenish subhedral grains up to 2 mm in size. The compositions of clinopyroxene phenocrysts lie within a wide Mg# range from 92 to 52 (Tables S3a, S3b, S3c, Suppl. 2). Most part (~ 90%) is represented by high-Mg clinopyroxenes (Mg# = 88–92). Variations of major components in clinopyroxenes from different sampling stations are close. The clinopyroxene phenocrysts show
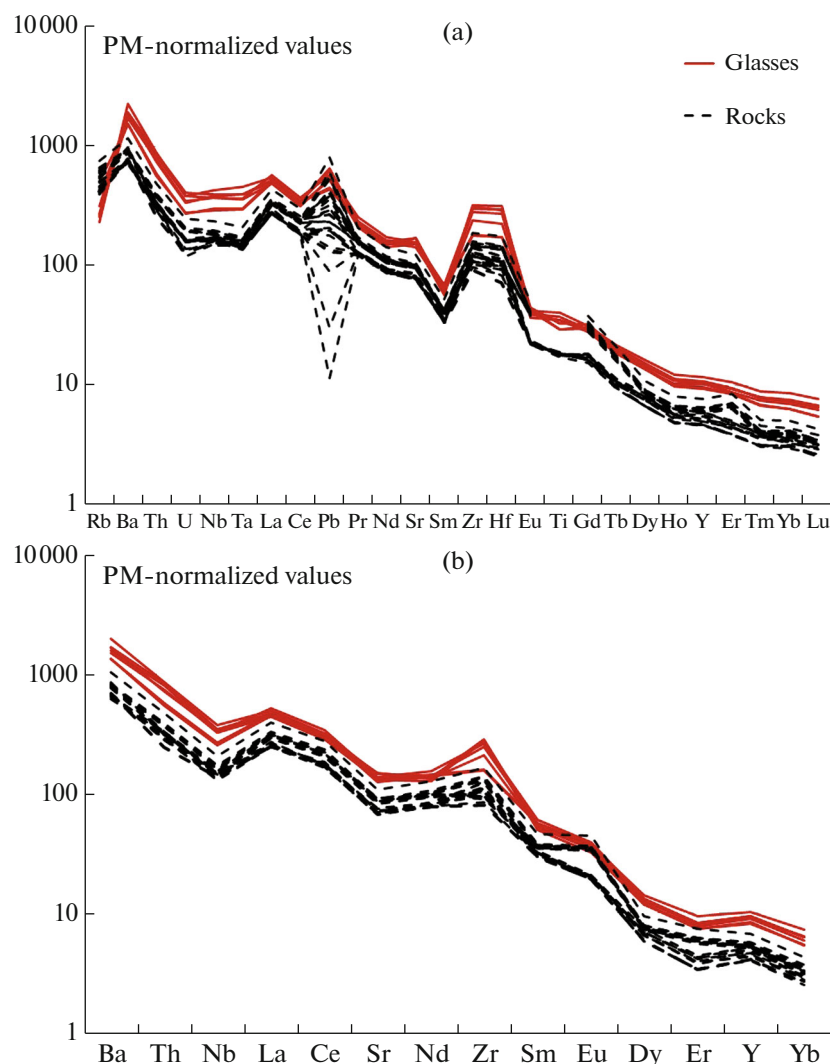
Fig. 7. Contents of lithophile and rare-earth elements in quench glasses and rocks of Mt. Gaussberg, normalized to primitive mantle (Sun and McDonough, 1989). Data on glasses are from this work. Data on rocks are taken from Sushchevskaya et al. (2014).

no zoning, but single grains contain core with elevated Fe and Al contents, which is surrounded by higher Mg rim (Fig. 3, Suppl. 1). Based on the characteristic differences in the content of some chemical elements, the clinopyroxenes are subdivided into two groups: group I is the main generation of clinopyroxene phenocryst and group II includes a few clinopyroxene grains that frequently compose central parts of large phenocrysts ("green cores") (Fig. 3). Group I consists mainly of high-Mg varieties (Mg# > 80, although some grains ascribed to this group have Mg# up to 69.5), with MgO content of 13−19 wt % and differs in the elevated contents of TiO_2 (from 0.6 to 1.7 wt %), Cr_2O_3 (from 0.05 to 1.2 wt %), NiO (0.02−0.07 wt %), and lowered contents of FeO (2.5−5 wt %) and Al_2O_3 (< 1.2 wt %). Group II is mainly represented by the lower Mg clinopyroxenes (Mg# 52−83) with MgO content from 10 to 16 wt %. It differs from group I in the elevated contents

of Al_2O_3 (from 0.7 to 4.5 wt %) and FeO (from 2 to 16 wt %) at lowered contents of TiO_2 (0.1−0.6 wt %), Cr_2O_3 (< 0.1 wt %), and NiO (< 0.02 wt %) (Fig. 11). The CaO concentrations in group I vary from 20.5 to 24 wt %; approximately the same range is typical of group II. The Na_2O contents in group I clinopyroxenes (0.05−0.50 wt % Na_2O) in general are lower than those of group II clinopyroxene (0.56−0.95 wt % Na_2O), reaching 1.2−1.8 wt % Na_2O in some grains (Fig. 11f). The average composition of group I clinopyroxenes recalculated for end members is expressed as $En_{50.7}Wo_{44.3}Fs_5$, while that of group II, is $En_{42.6}Wo_{41.4}Fs_{16}$ (Suppl. 2, Tables S3a, S3b). According to the modern classification (Morimoto et al., 1988), both clinopyroxene groups fall in the diopside field, although similar high-Fe cores in the previous mineralogical studies of the Gaussberg lamproites were termed salites
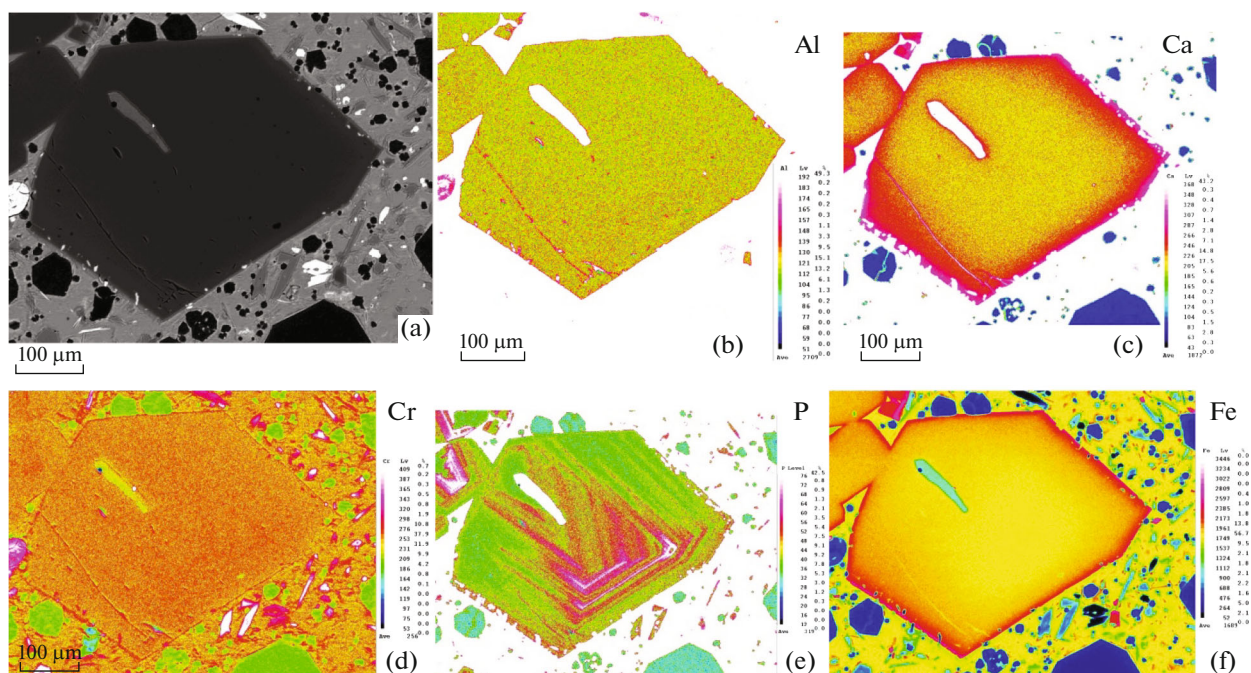
Fig. 8. Electron microprobe images of typical olivine phenocrysts from the Gaussberg lamproites (sample #469-4). (a) BSE image. (b–f) distribution maps of Al, Ca, Cr, Fe, and P. Olivine contains elongated glassy inclusion. High-resolution images are given in Supplementary 4.

according to the earlier classification (Foley and Jenner, 2004; Poldervvart and Hess, 1951).

Based on the major element composition, the group I clinopyroxenes from the Gaussberg lamproites are close in composition to the phenocrysts in high-K rocks of the Leucite Hills province, Wyoming, USA, and wyomingites of West Kimberly (West Australia) (Gupta and Yagi, 1980). Thereby, they differ from clinopyroxenes in Antarctic rocks (alkaline basalts of the Hobbs coast and flood basalts of the Queen Maud Land) have the lower Al_2O_3 content (Fig. 11a). Group II clinopyroxenes of Gaussberg in terms of Ti, Cr, and Al contents are closer to the fractionated compositions of clinopyroxenes of Antarctica (Figs. 11a, 11b).

The trace-element contents in the Gaussberg clinopyroxenes are listed in Table S3c (Suppl. 2). The content of trace elements in group II clinopyroxene principally differs from that of group I compositions, which once more confirms the absence of genetic relation between two groups of clinopyroxenes. Thereby, it should be noted that the clinopyroxene phenocrysts within group I are characterized by homogenous trace-element distribution, except for several analyses (Fig. 12). The contents of lithophile elements (e.g., Zr, La, V, Sc, Nb) in the clinopyroxene phenocrysts significantly correlate with each other, but correlation with major elements is not observed (Suppl. 3).

In terms of trace-element content, the Gaussberg clinopyroxenes principally differ from clinopyroxenes in other volcanic rocks of Antarctica. Compared to the clinopyroxenes from the flood basalts of the Queen Maud Land and alkaline basalts of the Hobbs coast (Migdisova et al., 2004), the Gaussberg clinopyroxenes have the higher MREE and lower HREE contents (Fig. 12). This peculiarity is likely related to the fact that in the ultra-alkaline rocks, site M2 in the crystal structure of clinopyroxene is greater than in the clinopyroxenes from basaltic melts, and, respectively, can be more easily occupied by highly incompatible elements with high ionic radius (Carbonin et al., 1989). The characteristic features of primitive mantle-normalized lithophile element patterns of group I clinopyroxenes of Gaussberg are Zr–Hf, Pb, and Ti minima and Eu, La–Ce, and Th maxima. The double Zr–Hf minimum could be related to the fact that the melts were oversaturated in alkalis, with which Zr and Hf could form complexes, thus preventing the incorporation of these elements in the clinopyroxene structure (Foley and Jenner, 2004; Ellison and Hess, 1994).

The trace element patterns of group II clnopyroxenes are peculiar in deep Sr and Ba anomalies, and high Th–U and Pb maxima at the absence of Zr–Hf minima and sharp HREE depletion, which are typical of other patterns of the Gaussberg clinopyroxenes. The normalized trace-element pattern of the Group II clinopyroxene is more similar to those of phenocrysts in flood basalts from the Queen Maud Land and alkaline basalts of the Hobbs coast (Migdisova et al., 2004) (Fig. 12).
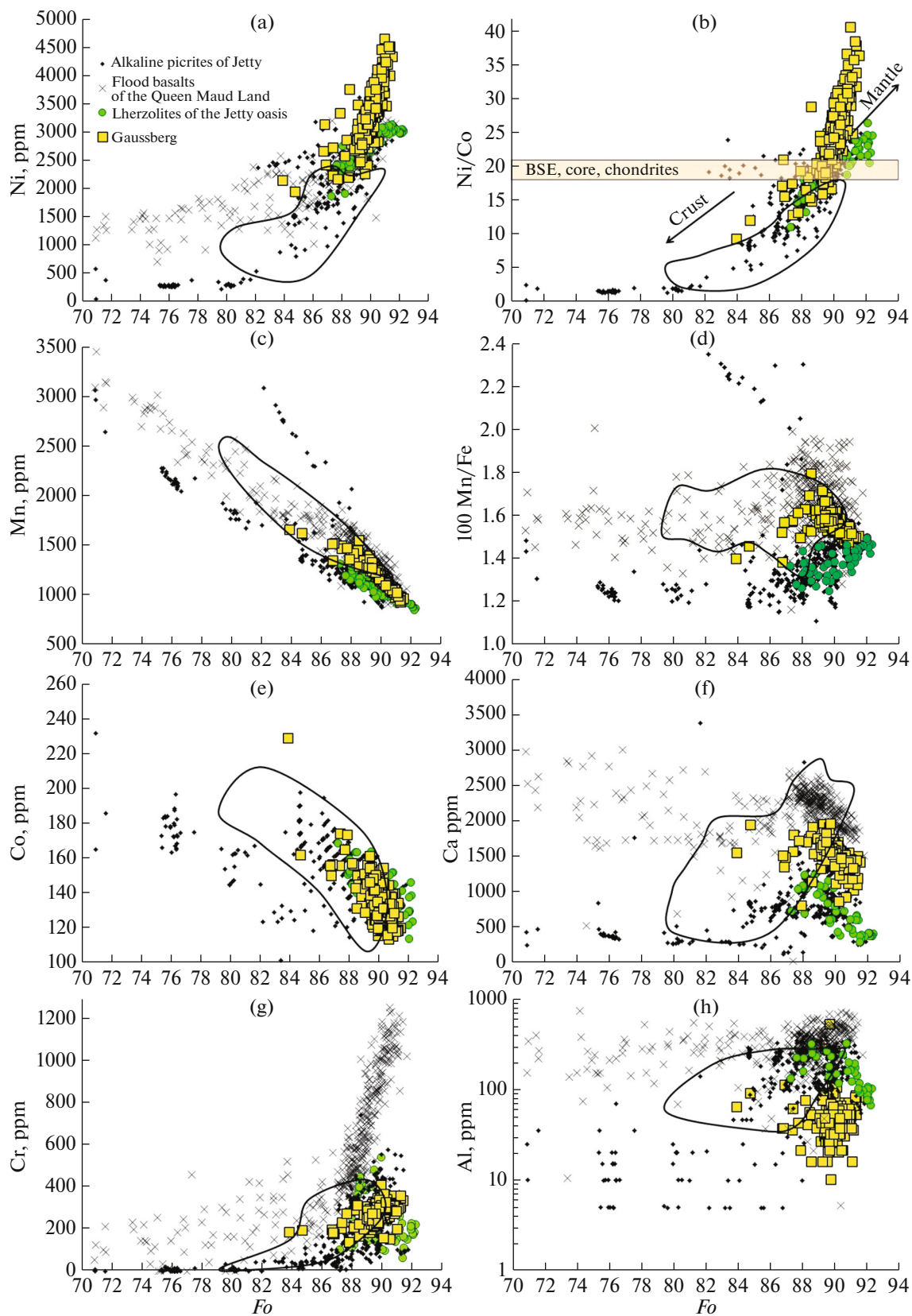
Fig. 9. Contents of Ni, Mn, Co, Cr, Ca, and Al and variations of characteristic Ni/Co and 100*Mn/Fe ratios versus forsterite component (Fo) in the olivine phenocrysts of the Gaussberg lamproites compared to the olivines of alkaline picrites and lherzolites of the Jetty Oasis (Sushchevskaya et al., 2018), tholeiites of South Atlantic (PetDB, shown as field), and flood basalts of the Queen Maud Land (Grantham et al., 1996). The values of Ni/Co ratio for BSE (Bulk Silicate Earth), core, and chondrites are given according to (Sobolev et al., 2007).
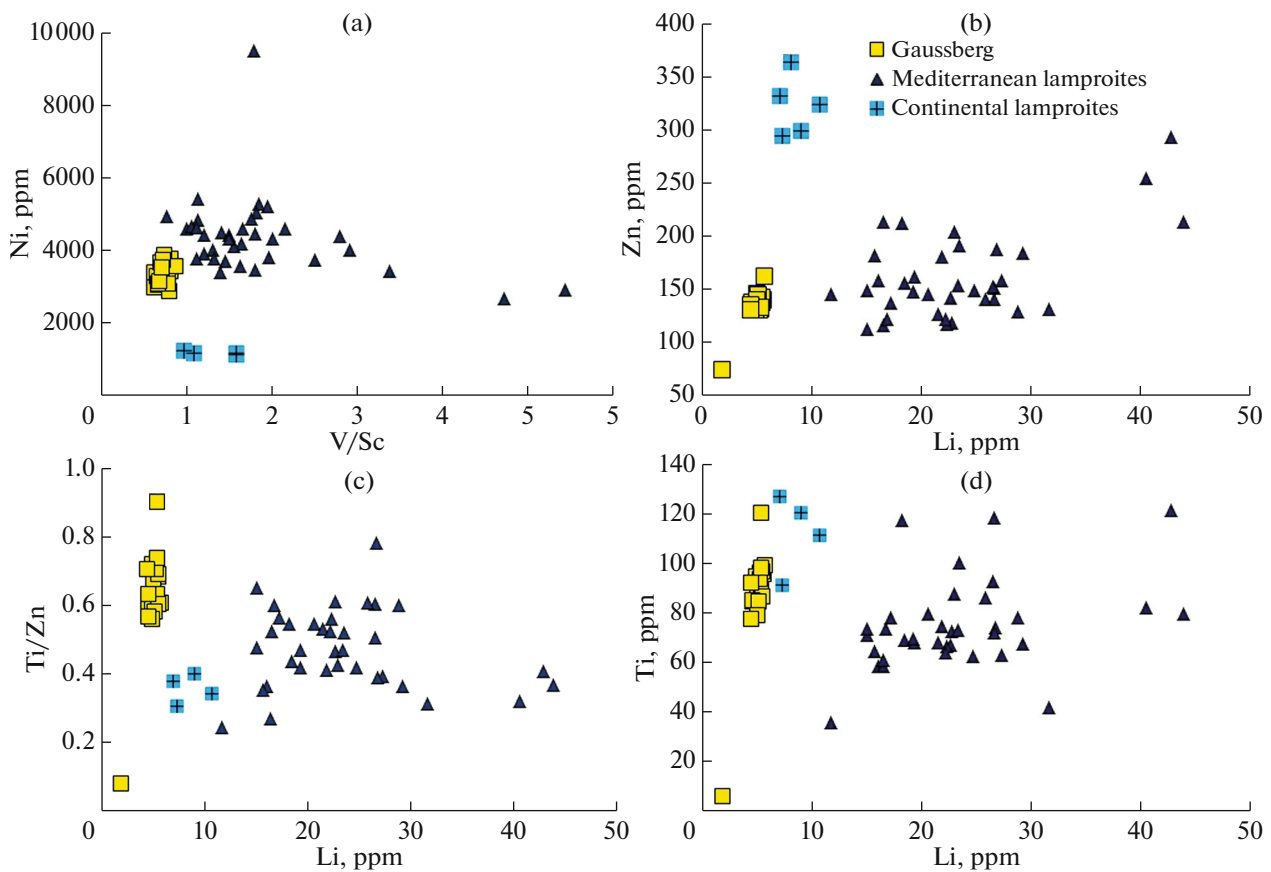
Fig. 10. Contents of Li, Zn, Ti and V/Sc ratios in olivine phenocrysts of the Gaussberg lamproites compared to those of olivines from lamproites of the Mediterranean belt (Mediterranean lamproites (Prelevic and Foley, 2007), continental lamproites (Prelevic et al., 2013)).

Two clinopyroxene groups, "salite" or "green cores" with elevated FeO, Al_2O_3, and Na_2O contents and light colored phenocrysts of low-Fe diopsidic clinopyroxene, were previously distinguished in the Gaussberg lamproites and other ultrapotassic volcanic rocks (Gupta, 2015). Foley (1985) and Foley and Jenner (2004) described that some clinopyroxene phenocrysts of Gaussberg contain corroded salitic green cores, which are surrounded by diopside shell. The compositions of these green cores correspond to those of group II distinguished in our work (Fig. 11). The bright green clinopyroxene phenocrysts with elevated Al, Fe, and sometimes Na contents were found also in the Shiprock lamproites (USA) (Wagner and Velde 1986), Leucite Hills (USA) (Barton and van Bergen, 1981), ultrapotassic rocks of Italy and Greece (Barton et al. 1982; Pe-Piper, 1984), and other volcanic rocks (Jankovics et al., 2016; Geng et al., 2022). In terms of composition, the clinopyroxene phenocrysts and "green cores" from leucitites of the Leucite Hills Province are close to groups I and II of Gaussberg, respectively (Fig. 11).

Leucite

Fresh unaltered leucites in the lamproitic rocks are extremely scarce. During secondary alterations, they are usually replaced by sanidine, analcime, quartz, carbonates, and zeolite (Gupta, 2015). However, leucite phenocrysts in the Gaussberg rocks are mainly represented by unaltered well-shaped crystals, which could contain glassy and fluid inclusions. However, some samples contain large leucite grains (up to 2 mm) of irregular shape with traces of secondary alterations, which was previously mentioned in (Foley, 1985; Foley and Jenner, 2004) (Fig. 2f; Suppl. 1). The phenocrysts show no zoning, but reveal twinning related to the leucite transition from cubic to tetragonal syngony at ~690°C (Peacor, 1968; Henderson and Taylor, 1969).

In this work, we obtained ~ 550 analyses of leucite grains in the Gaussberg lamproites (Suppl. 2, Table S4). The composition of the Gaussberg leucites corresponds to the ideal leucite stoichiometry of $K[AlSi_2O_6]$. The leucites are enriched in Na_2O (0.05–0.35 wt %), but are depleted in K_2O (19.9 to 20.9 wt %) and are characterized by the lowered K_2O/Al_2O_3 compared to leucites from lamproites of the Leucite Hills (USA) and West Kimberly (Africa) provinces (Jaques et al., 1986; Mitchell and Bergman, 1991) (Fig. 13). The BaO and SrO contents in the leucite phenocrysts of Gaussberg reach 0.3 and 0.04 wt %, respectively. The determination of contents of other trace elements, for instance,
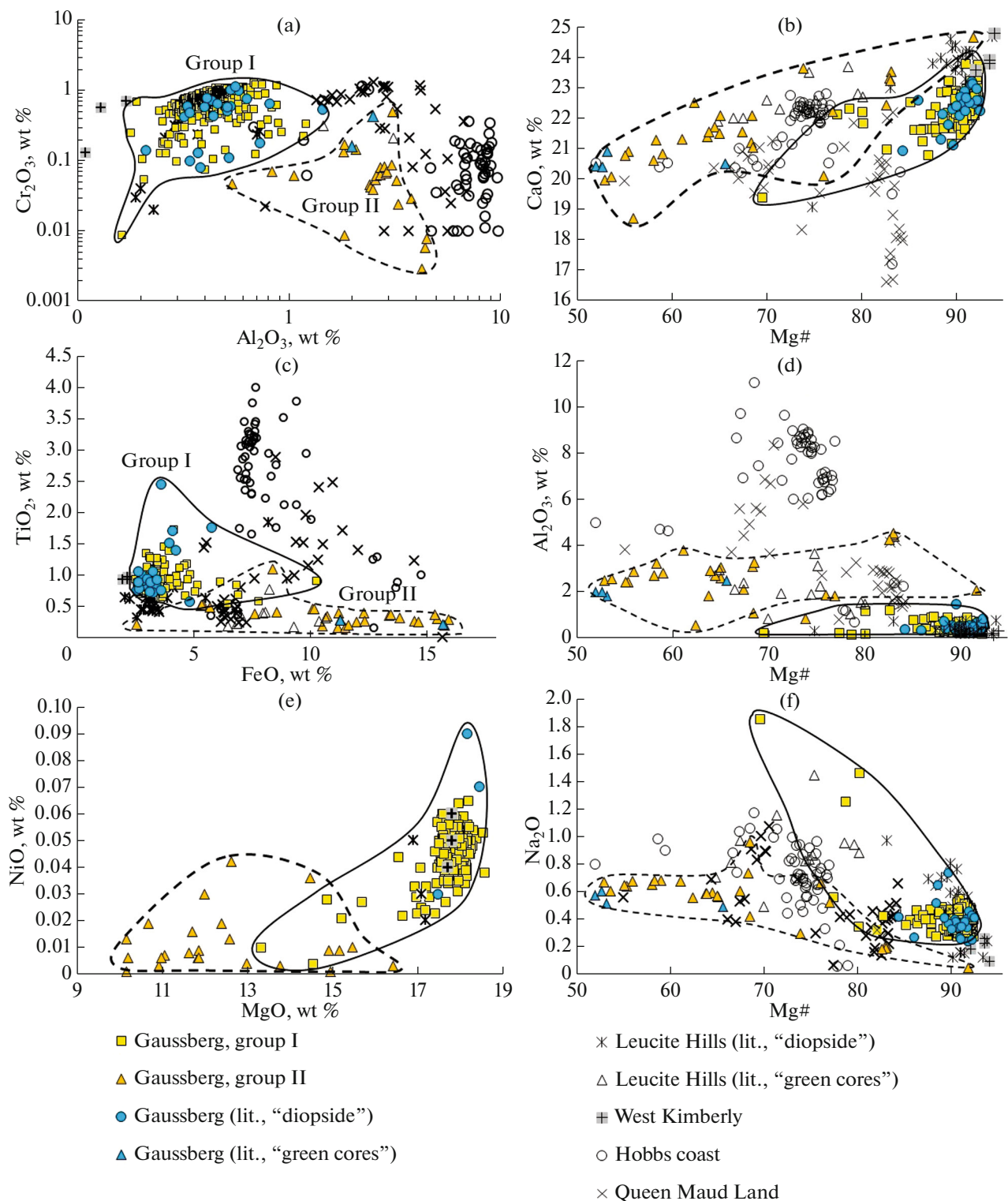
Fig. 11. Variations of major oxides and magnesium number (Mg# = 100(MgO/40.319)/((MgO/40.319) + (FeO/71.847)) for clinopyroxenes from the Gaussberg lamproites according to our and literature data ("diopside"—Foley, 1985; Foley and Jenner, 2004; Salvioli-Mariani, 2004). Based on our studies, the compositions of group I and II phenocrysts were distinguished in the Gaussberg lamproites. Shown are compositions of clinopyroxene "green cores" in the Gaussberg lamproites according to (Foley, 1985; Foley and Jenner, 2004). Compositions of clinopyroxene phenocrysts in the alkaline basalts of the Hobbs area, alkaline basalts of Antarctica, Mesozoic flood basalts of the Queen Maud Land (Hart et al., 1997; Migdisova et al., 2004), and wyomingites of West Kimberly (West Australia) (Gupta and Yagi, 1980) and Leucite Hills (Wyoming, USA) (Gupta and Yagi, 1980; Barton and Bergen, 1981) are shown for comparison. Compositions of the main group of clinopyroxene phenocrysts ("diopside") and "green cores" of clinopyroxenes (Barton and Bergen, 1981) for Leucite Hills leucitites (Barton and Bergen, 1981) are shown separately.
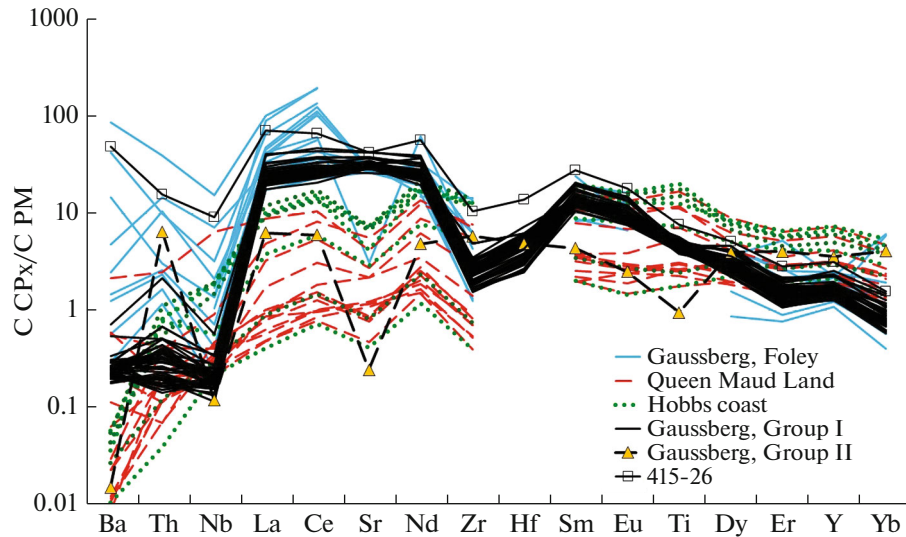
Fig. 12. Distribution of trace and lithophile elements in clinopyroxene phenocrysts from the Gaussberg lamproites according to data from this work and Foley and Jenner (2004). Distinguished are values for groups I and II clinopyroxenes, while analysis of grain 475-26 ascribed to group I is shown separately. Data on the clinopyroxene phenocrysts of the Antarctic alkaline province: Hobbs coast and Mesozoic flood basalts of the Queen Maud Land (Migdisova et al., 2004). Concentrations of elements are normalized to the primitive mantle after (Sun and McDonough, 1989).

REE, in the leucites is complicated by their extremely low contents, which is explained by their too large sizes to be incorporated into crystal lattice (Foley and Jenner, 2004).

According to our and literature data, the Gaussberg leucites can be subdivided into three groups based on Fe composition (Fig. 13). Data points of leucites that compose the central parts of phenocrysts form a field with Fe_2O_3 contents within 0.7−1.2 wt %, but some grains contain Fe content less than 0.45 wt % Fe_2O_3 or are highly enriched in iron (1.2−2.0 wt % Fe_2O_3). According to Foley (1985), the Gaussberg lamproites contain two leucite generations: earlier generation represented by resorbed grains with lowered Fe_2O_3 (<0.3 wt %) and generation of typical leucite phenocrysts with Fe_2O_3 content more than 1 wt %. According to (Salvioli-Mariani et al., 2004), the phenocrysts form a cluster with low Fe_2O_3 content, while Fe-rich leucites in the Gaussberg lamproites (1.3−2.4 wt % Fe_2O_3) occur as microlites in the groundmass and as thin rims around phenocrysts (Fig. 13).

The Fe_2O_3 content in the Gaussberg phenocrysts is close to that of the West Kimberly leucites, but is lower than in the alkaline rocks of the Leucite Hills province (Jaques et al., 1986; Mitchell and Bergman, 1991). The Fe_2O_3, Na_2O, and K_2O contents show no systematic variations with SiO_2 content in leucite phenocrysts, which would be observed at crystallization differentiation. It should be noted that the low-Fe group of the leucite grains of Gaussberg differs also in the lowered SiO_2 and elevated K_2O contents compared to typical phenocrysts (Fig. 13).

Chromian Spinel

The analyzed compositions of spinel inclusions in olivine phenocrysts (Fo_{89-90}) vary within a more narrow range than those determined in (Foley, 1985) (Fig. 14; Suppl. 2, Table S5). The Mg# (Mg# = $100Mg/Mg + Fe^{2+}$) of spinel varies from 57 to 51, while the fraction of ferric iron (Fe^{3+}# = $100 \cdot Fe^{3+}/(Fe^{3+} + Fe^{2+})$) varies from 29 to 37 (on average, 34). These values are lower than previously revealed Fe# ~ 40 for the same Mg# range (Foley, 1985). The chrome number (Cr# = $100Cr/(Cr + Al + Fe^{3+})$) coincides with the previously published data and accounts for 84−77 (Foley, 1985). The Cr_2O_3 contents vary from 50 to 60 wt % with decreasing Mg# of spinel, whereas the contents of Al_2O_3 (on average, 3 wt %), MnO (0.23−0.31 wt %), NiO (0.2−0.25 wt %), and V_2O_3 (0.08−0.14 wt %) do not depend on the MgO concentrations. The TiO_2 content (24−28 wt %) positively correlates with FeO (4.2−1.9 wt %) and negatively, with Mg# (Fig. 14). The Cr_2O_3 concentration has a negative correlation with Al_2O_3: with increasing Cr # of spinel, the Al_2O_3 contents decrease, which is typical of magmatic spinel (Sigurdsson, 1977).

CRYSTALLIZATION OF THE GAUSSBERG MAGMAS

Order and Conditions of Crystallization of the Gaussberg Lamproites

Our and previous petrographic investigations of the Gaussberg lamproites showed that early crystallizing phases are magnesian olivines and clinopyroxenes, as
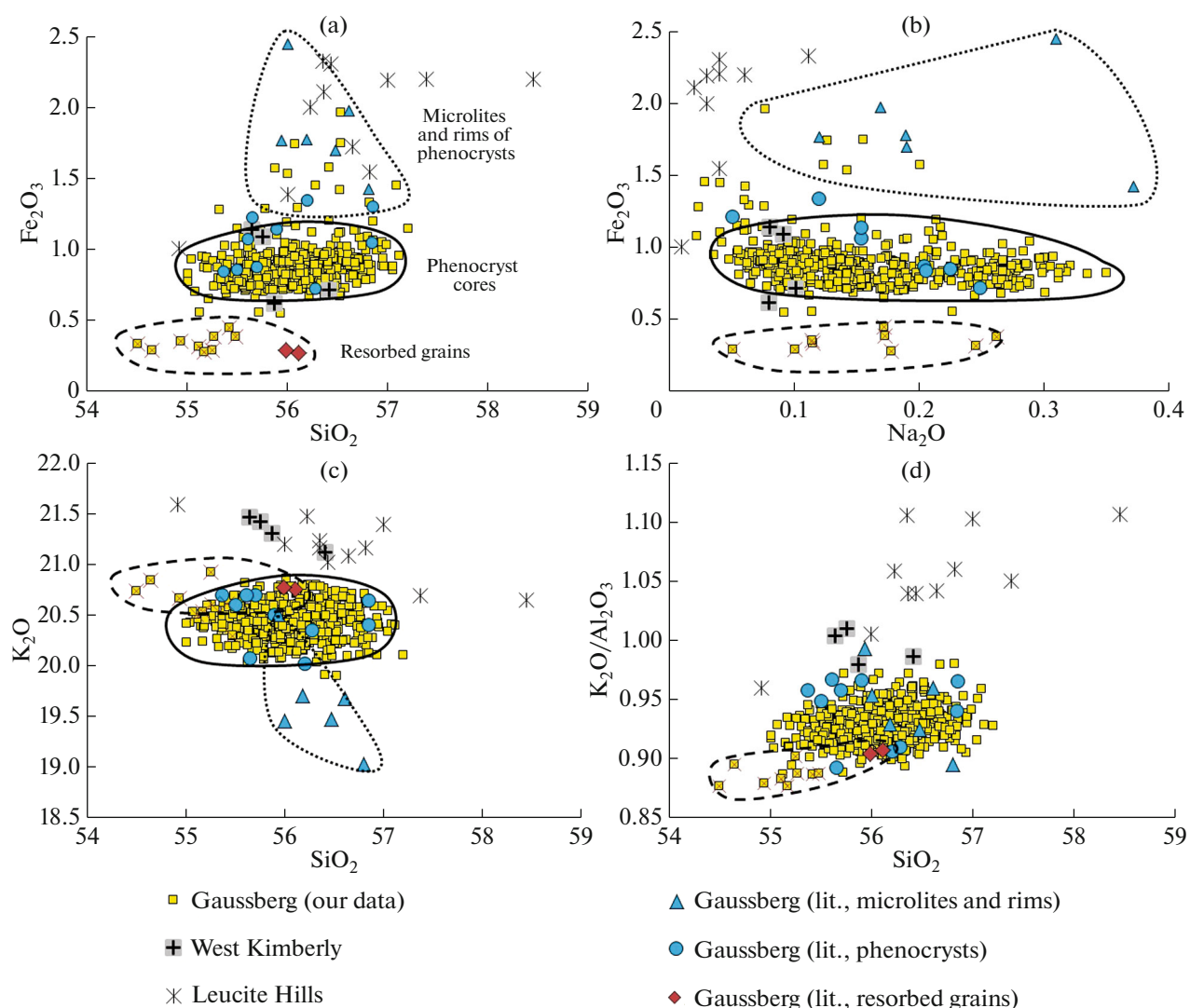
Fig. 13. Variations of oxides (in wt %) and K_2O/Al_2O_3 ratio in leucite phenocrysts from Gaussberg rocks compared to leucites from lamproites of the West Kimberly provinces (Africa) (Jaques et al., 1986; Mitchell and Bergman, 1991) and Leucite Hills (Wyoming, USA) (Mitchell and Bergman, 1991). For Gaussberg our and literature data are presented (Foley, 1985; Foley and Jenner, 2004, and Salvioli-Mariani et al., 2004), which are subdivided into three groups: phenocryst cores, resorbed low-Fe grains, as well as high-Fe microlites and rims of phenocrysts. Symbols of our compositions noted by diagonal crosses correspond to low-Fe leucite grains.

well as leucite, which form phenocryst assemblage (Vyalov and Sobolev, 1959; Sheraton and Cundari, 1980; Foley and Jenner, 2004). Thereby, the first liquidus phase of the Gaussberg lamproites is chromian spinel, which occurs as inclusions in olivine phenocrysts (Fo_{89-90}) (our data, Foley, 1985). The groundmass assemblage includes clinopyroxene, leucite, phlogopite, and apatite.

Phenocrysts in the Gaussberg lamproites form separate grains of euhedral and subhedral habit, but some grains form glomerophorphyric intergrowths (Figs. 2c, 2d; Suppl. 1). Vyalov and Sobolev (1959) found an olivine crystal surrounded by clinopyroxene crystals, which indicates the earlier crystallization of olivine.

The absence of characteristic petrographic evidences does not allow us to reconstruct exactly the crystallization order of phenocrysts based on the study of natural samples. In this case, important information can be obtained from experimental studies of lamproitic magmas carried out under controlled conditions. There are numerous experimental works on study of phase equilibria in the ultra-potassic magmatic systems, but only few experimental data are available on the Gaussberg lamproitic magmas (Gupta, 2015).

Experimental studies of crystallization of the Gaussberg lamproite melt were carried out at atmospheric pressure and different redox conditions by (Foley, 1985). It was shown that at crystallization of melt corresponding to the average bulk composition of
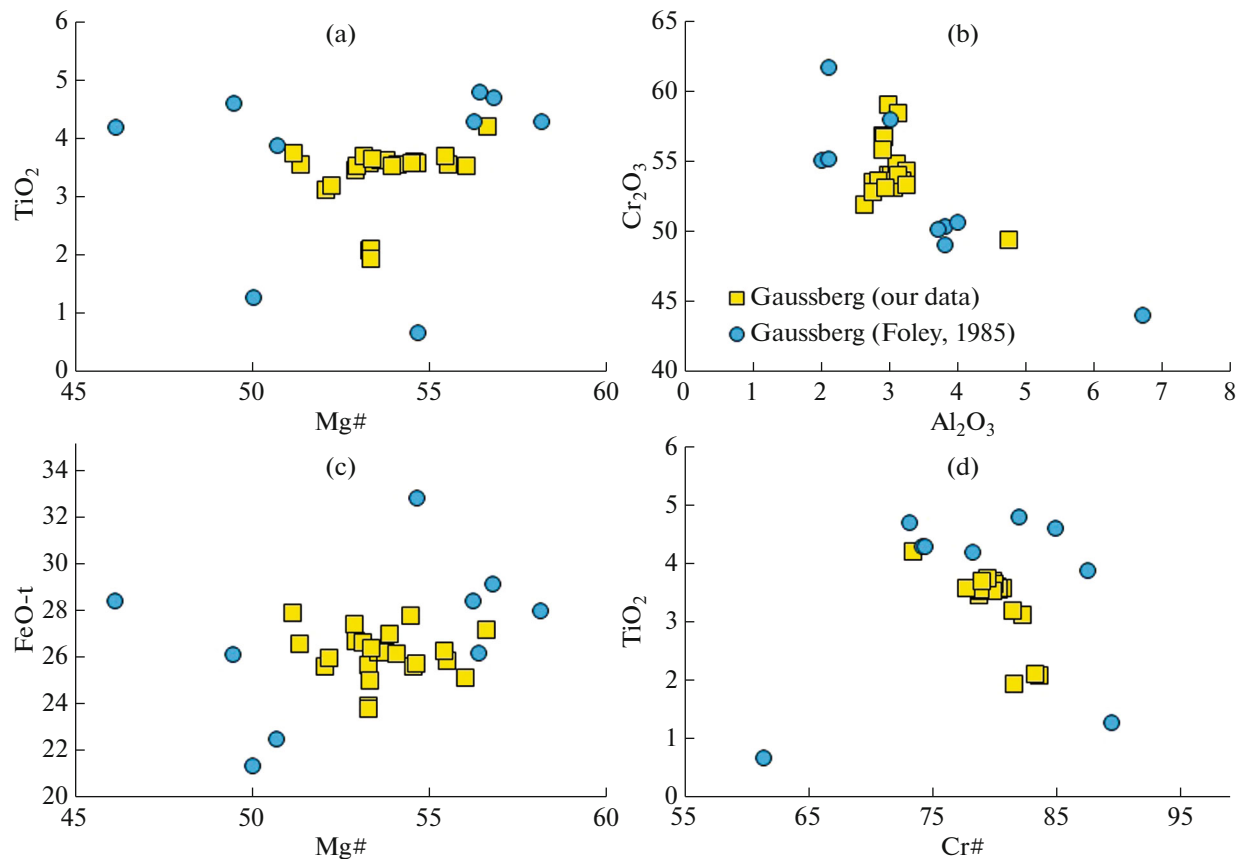
Fig. 14. Compositions of spinel inclusions in olivine phenocrysts from the Gaussberg lamproites according to our data and data from (Foley, 1985). Oxide contents are given in wt %.

the Gaussberg lamproites under NNO (nickel−bunsenite) or MW (magnetite−wustite) oxygen fugacity, the first liquidus phase is olivine at 1260°C, which with decreasing temperature by 10−20°C is appended by leucite. Crystallization of clinopyroxene and chromian spinel started at lower temperatures (<1200°C). It should be noted that under more oxidized conditions (at HM (hematite−magnetite) and MnH (manganosite−hausmannite) buffers), crystallization of olivine and leucite from the melt began simultaneously at 1260°C. The appearance of chromian spinel as the first liquidus phase (at 1280°C) in experiments (Foley, 1985) was attained by the addition of 0.2 wt % Cr_2O_3 in a starting composition. In these experiments, crystallization of olivine together with leucite and chromian spinel began at 1260°C within the entire studied redox interval (from MW to HM). Inasmuch as experimental series was carried out within a narrow (near-liquidus) temperature range, the appearance of clinopyroxene expected at lower temperature was not noted.

Phase equilibria in the forsterite + diopside + leucite ($Fo−Di−Lc$) synthetic system ($Fo−Di−Lc$) was studied in works by Gupta (1972) and Nag et al. (2007). Dry experiments under atmospheric pressure showed that the crystallization of melt in the Fo−Di−Lc system from starting composition $Fo_{15}Di_{40}Lc_{45}$, which

is close to the normative composition of the Gaussberg lamproites, follows the sequence: $Ol \rightarrow + Lc \rightarrow Ol + Lc + CPx$ (with presence of significant amount of residual melt) (Gupta, 1972). Under these conditions, the simultaneous crystallization of three phases occurs at $1296 \pm 3°C$ (normative composition of $Fo_3Di_{60}Lc_{37}$). In the water-saturated $Fo−Di−Lc$ system at pressure of 100 MPa, simultaneous crystallization of three mineral phases occurred at a temperature of $880 \pm 5°C$, which is almost 400°C lower than that of the dry system at atmospheric pressure (Nag et al., 2007). Thereby, the position of this point is shifted toward leucite, thus reflecting a decrease of the stability field of this mineral to the water-saturated system ($Fo_3Di_{50}Lc_{47}$) (Nag et al., 2007). It should be noted that at given conditions (water-saturated system at 100 MPa), the further temperature decrease to $850 \pm 10°C$ leads to the phlogopite crystallization simultaneously with olivine, leucite, and clinopyroxene (Nag et al., 2007).

Experiments performed in the $Fo−Di−Lc$ system at pressure of 2.3 GPa and water-saturated conditions showed that leucite is not crystallized at relatively high pressure. Instead, phlogopite, kalsilite, and K-feldspar become stable under these conditions (Nag et al., 2007). Previously, the experimental study of the $K_2O−Al_2O_3−SiO_2$ system showed that at dry conditions and

temperature of 1250°C, leucite is stable at pressures below ~2 GPa, whereas at higher pressure, leucite is decomposed into feldspar and kalsilite. At lower temperatures, the pressure stability field of leucite becomes narrower (Fasshauer et al., 1998). Under water-saturated conditions, leucite is stable only at pressure below 0.5 GPa (Tuttle and Bowen, 1958; Morse, 1969).

Thus, the existing experimental data show that the crystallization of olivine + leucite + clinopyroxene assemblage from high-K melts is possible within sufficiently wide range of redox conditions (from MW to MH), while crystallization temperature strongly depends on the water presence in the system. Thereby, the leucite stability is constrained by pressure below 2 GPa in dry systems and < 0.5 GPa in the water-saturated systems.

The liquidus temperatures of the Gaussberg primitive magmas were estimated using composition of equilibrium pairs of spinel inclusions in olivine phenocrysts Fo_{89-91}. Application of the thermometer based on the Al_2O_3 distribution between olivine and spinel (Coogan et al., 2014) yielded the temperature range $T = 1180-1250°C$. Method by Ballhaus et al. (1991) gave even lower estimates of liquidus temperatures of $1086-1219°C$ (Suppl. 2, Table S5).

Previously, the crystallization temperature of the Gaussberg lamproite magmas was estimated by study of melt inclusions in olivine and leucite in two samples of the Gaussberg lamproites (Salvoli-Mariani et al., 2004). Microthermometric studies showed that the complete melting of glass in the inclusions occurs within 1070−1140°C, but shrinkage bubble did not disappear. Melting of host leucite began at 1213−1238°C. These authors (Salvoli-Mariani et al., 2004) also calculated the crystallization temperature of olivine based on the Fe−Mg partition coefficient between olivine and liquid using equation of Ford et al. (1983). The Fe^{3+}/Fe^{2+} ratio was calculated using the estimated redox conditions of crystallization of the Gaussberg lamproites at NNO−0.5, obtained in experimental work (Foley, 1985). The equilibrium temperatures of melt inclusions with host olivine calculated using this technique are within 1103−1158°C (Salvoli-Mariani et al., 2004). The temperature ranges obtained by studying melt inclusions are below experimentally determined values at dry conditions (Foley, 1985; Gupta et al., 1972), which may indicate that crystallizing magma contained water that caused a decrease of liquidus temperature (Nag et al., 2007). The low water content (0.7 wt % H_2O) in the Gaussberg quench glasses as well as the presence of CO_2-bearing fluid in quench bubbles of melt inclusions have been previously demonstrated for the Gaussberg lamproites (Salvoli-Mariani et al., 2004). The presence of water accumulating during magma fractionation is also confirmed by the crystallization of phlogopite microlites in the groundmass (Fig. 2b).

Oxidation conditions of the Gaussberg lamproites at ~ NNO buffer (which corresponds to ~QFM + 0.7) were obtained in (Foley, 1985) based on the experimental data and compositions of natural minerals. The author noted the high Fe_2O_3 contents in leucite phenocrysts (up to 2 wt %) and the elevated Fe# in spinel inclusions in olivine phenocrysts (~34). Foley (1985) also reported that leucite is represented by two generations with different Fe^{3+}: the earlier leucite generations are significantly depleted in Fe^{3+} (~ 0.3 wt % Fe_2O_3) compared to the late generation, which suggests a change of oxygen fugacity from lower fO_2 below MW buffer to NNO (~QFM + 0.7), i.e., magma oxidation en route to the surface (Foley, 1985). Our study based on the analysis of over 500 grains and petrographic observations showed that typical leucite phenocrysts contain 0.7−1.2 wt % Fe_2O_3, while low-Fe grains occur rarely, in some samples, as altered partly resorbed grains, sometimes in intergrowths with green clinopyroxene (Figs. 13, 2e). Additional studies are required to understand whether these low-Fe leucites are the products of crystallization of the Gaussberg lamproite magma at more reducing conditions. Salvoli-Mariani et al. (2004) showed that the elevated Fe content is observed in leucite microlites from the groundmass and thin rims around phenocrysts, and likely corresponds to the more oxidized conditions during ejection of the Gaussberg lamproitic magmas.

We estimated the redox crystallization conditions of the Gaussberg lamproites using several techniques. The calculations using olivine−spinel oxybarometer (Ballhaus et al., 1991) correspond to the relatively oxidized conditions within the range from QFM + 1.3 to QFM + 2.3 (Suppl. 2, Table S5). Using olivine−spinel oxybarometer (Nikolaev et al., 2016) yielded estimates from QFM + 0.9 to QFM + 1.9. Estimates obtained using oxybarometers based on the vanadium partitioning between coexisting olivine and melt (Canil and Fedortchouk, 2001; Mallmann and O`Neill, 2013; Shishkina et al., 2018) also show the more oxidized crystallization conditions of magmas compared to Foley data (Foley, 1985) within the range from QFM− 0.5 to QFM + 1.2 (Mallmann and O`Neill, 2013) or from QFM + 1.4 to QFM + 3.5 (Canil and Fedortchouk, 2001; Shishkina et al., 2018). Model of Mallmann and O`Neill (2013), unlike the models by Shishkina et al. (2018) and Canil and Fedortchouk (2001), takes into account the effect of presence of alkalis (K_2O and Na_2O) in melt, which is principal for the Gaussberg ultra-potassic lamproites (Shishkina et al., 2023).

Thus, a complex study of natural samples in combination with experimental data on phase equilibria makes it possible to reconstruct the main trends in the crystallization conditions of the Gaussberg lamproite magmas. The first crystallizing phase is chromian spinel, which occurs as inclusions in high-Mg olivine crystals. The chromian spinel+olivine assemblage could crystallize within a temperature range from 1180

to 1250°C. Further crystallization of magma with formation of phenocryst assemblage in order of olivine → olivine + leucite → olivine + leucite + clinopyroxene and with capture of melt inclusions could occur at lower temperatures within 1070−1140°C, which correspond to the water presence in the system. The phenocryst assemblage in the Gaussberg lamproites likely crystallized in a shallow chamber (below ~500 MPa), which corresponds to the leucite stability field in the water-bearing systems (Tuttle and Bowen, 1958; Morse, 1969). Crystallization of microlite assemblage of clinopyroxene + leucite + phlogopite at quenching lamproite magma corresponds to the experimental observations at lowered temperatures (<850°C) in the water-saturated system at 0.1 MPa (Nag et al., 2007). Performed calculations show that lamproites could crystallize within a wide range of redox conditions from QFM−0.5 to QFM + 2.3, which is consistent with existing experimental data (Foley, 1985). Differences in estimates of redox conditions of crystallization of the Gaussberg ultra-alkaline magmas based on the existing oxybarometers show that these techniques are poorly applied to highly alkaline melts and require special calibrations.

Presence of "Exotic" Clinopyroxene and Leucite Phenocrysts

Based on the appearance and compositional peculiarities, some clinopyroxene and leucite phenocrysts principally differ from the main phenocryst generation of the Gaussberg lamproites and rather crystallized from other magma portions and at different physicochemical conditions. The presence of aggregates or intergrowths of resorbed leucite grains (up to 2 mm) and green clinopyroxene crystals in some samples may indicate their simultaneous crystallization (Fig. 2f; Suppl. 1).

These minerals include group II clinopyroxene phenocrysts, which usually compose resorbed or fused "green cores". They are peculiar in the elevated contents of Al_2O_3, FeO, and Na_2O at lowered contents of TiO_2, Cr_2O_3, and NiO and differ from typical clinopyroxene phenocrysts of Gaussberg (group I) in the trace element composition (Figs. 11, 12).

The elevated Na and Al contents in the clinopyroxene could reflect the relatively high pressure during their crystallization (Thompson, 1977). The fact that the Gaussberg clinopyroxene phenocrysts contain high-Al cores and low-Al rims suggests two levels of magma crystallization during ascent to the surface. However, separation of two clinopyroxene groups of Gaussberg based on Ti, Cr, and Ni contents and significant differences in the trace element composition exclude their crystallization from portions of related magma. Principally different contents of trace elements in group II clinopyroxenes indicate that they cannot be in equilibrium with melts of the main group, which formed the upper part of Gaussberg volcano. It

is possible that lavas ejected at the earlier stages are absent in the upper part of the volcanic edifice. The presence of "salite" phenocrysts in the ultra-potassic rocks, including the Gaussberg lamproites, could be explained by different mechanisms. They could be xenocrysts captured by the Gaussberg lamproitic magma from defragmented clinopyroxene-bearing nodules (Barton and van Bergen, 1981) or obtained through mixing of two different magma types (Barton et al., 1982). At the same time, complex geochemical studies, including isotopic composition of clinopyroxene, of the primitive basalts in the northern China Craton showed that the "green cores" of clinopyroxenes crystallized from differentiated portions of the main basaltic magma (Geng et al., 2022). It was demonstrated (Jankovics et al., 2016) that the clinopyroxene "green cores" in the alkaline basalts of the Carpathians−Pannonian regions are subdivided into different generations: xenocrysts entrapped from host mafic granulites and phenocrysts formed at different stages of magma evolution (Jankovics et al., 2016).

Among numerous leucite grains studied in the Gaussberg lamproites, a group can be distinguished that sharply differs from most typical phenocrysts. It is represented by large grains (up to 2 mm) with traces of resorption and secondary alterations (Fig. 2f; Suppl. 1). These leucites differ in the lowered contents of Fe and Si and the elevated contents of K compared to typical leucites. The presence of two leucite generations in the Gaussberg lamproites allowed Foley (1985) to suggest a change of oxygen fugacity in the system. The low-Fe leucite (earlier generation) has crystallized under more reduced conditions (much below the NNO buffer). At the late stages, when magma approached the surface, the main group of phenocrysts crystallized under more oxidized conditions (at NNO buffer) (Foley, 1985). The crystallization of high-Fe leucite microlites and rims around phenocrysts marks the more oxidized conditions during magma ejection on the surface.

The question of origin of "green cores" of the group II clinopyroxene with elevated contents of Al, Fe, and Na and low-Fe leucite grains in the Gaussberg lamproite magmas requires additional study.

Trace Element Partitioning between Olivine and High-K Melt

The contents of trace elements in the olivine phenocrysts of magmatic rocks are sufficiently low (Table S2, Suppl. 1), except for Ni and Mn, concentrations of which could exceed 1000 ppm. The sizes of most cations of incompatible elements are too large to be incorporated easily in M1 and M2 sites having close sizes. The incorporation in structure of Zr^{4+}, Sc^{3+}, and Li^{1+} of suitable size requires charge compensation, which leads to their lowered concentrations in olivine (Kohn and Schofield, 1994). Conditions of generation and crystallization also affect the entrapment of trace

components in olivine crystals. The trace element partition coefficients in olivine increase with melt differentiation at decreasing temperature, decrease of MgO contents, and the growth of SiO_2 concentrations (Kohn and Schofield, 1994).

Nickel is the most compatible trace element in olivine. As shown by Koshlyakova et al. (2022) based on analysis of the existing experimental data, the nickel partition coefficient $\left(D_{Ni}^{Ol/M}\right)$ strongly depends on the melt composition and temperature (T). Thereby, both T and alkali contents (Na and K) in the melt have a negative correlation, whereas SiO_2 content in the melt has a positive correlation with $D_{Ni}^{Ol/M}$. An increase of SiO_2 content leads to the greater polymerization of the melt and decrease of NBO/T (ratios of non-bridging oxygens to the number of tetrahedrally coordinated cations). In contrast, the K^+ and Na^+ are modifier cations and prevent melt polymerization, forming the great number of non-bridging oxygens and thus increasing NBO/T (Mysen and Richet, 2018). Previously, a negative correlation between NBO/T melt and $D_{Ni}^{Ol/M}$ was demonstrated in (Mysen and Virgo, 1980). Based on experimental data, Koshlyakova et al. (2022) suggest that a negative effect of K content in the melt is higher than that of Na, which is of great significance for lamproitic rocks.

It was assumed (Foley and Jenner, 2004) that the nickel partition coefficient depends on the melt alkalinity, and $D_{Ni}^{Ol/M}$ increases with the growth of alkalinity and can reach 60−80 in the ultra-alkaline melts (Foley and Jenner, 2004). The values of nickel partition coefficients between olivine and mafic melts determined in experimental studies lie between 2 and 20 (Koshlyakova et al., 2022). Thereby, the highest $D_{Ni}^{Ol/M M}$ obtained in experiment with mafic melt (54 wt % SiO_2, 12 wt % MgO, 2.7 wt % Na_2O) at temperature 1250°C is 48 (Duke, 1976). The values of $D_{Ni}^{Ol/M}$ calculated in (Shishkina et al., 2023) from the bulk compositions of lamproites and olivine phenocrysts are 11−21, whereas coefficients calculated from compositions of quench glasses vary within 53−153. In (Foley and Jenner, 2004), the values of $D_{Ni}^{Ol/M}$ calculated from compositions of quench glasses varied within 62−95 (on average, 82). Calculations conducted using the model by Koshlyakova et al. (2022), which takes into account the effect of not only temperature but also the contents of alkaline elements in melt, showed that the $D_{Ni}^{Ol/M}$ value for the Gaussberg lamproitic melts is 27. In our opinion, the high nickel partition coefficients for olivine obtained by (Foley and Jenner, 2004) are explained by incorrect choice of the melt composition. The quench glasses of the Gaussberg lamproites are differentiated melt portions that are disequilibrium with high-Mg olivines, which is confirmed by KD_{Ol-Mel}^{Fe-Mg}t values within

0.10−0.15, which do not correspond to equilibrium (Toplis, 2005).

The trace element partition coefficients between olivine and Gaussberg primitive melt were determined in (Shishkina et al., 2023) compared to data on the island arcs and mid-ocean ridge basalts. Note that the $D_{element}^{Ol/M}$ values in the Gaussberg olivines are close to those of ugandites of the Bunyaruguru volcanic field and leucite basanites of the Virunga volcanic field (Foley et al., 2011).

In spite of the negative effect of alkali contents in the melt on $D_{Ni}^{Ol/M}$, olivines from ultra-alkaline magmas show the highest Ni contents, which could be caused by different reasons, and, first of all, by high Ni contents in the magma generation source (Davis and Smith, 1993), for instance, owing to the involvement of pyroxenite-bearing mantle source.

Origin of Ultra-Potassic Lamproites of Gaussberg Volcano

It is generally accepted that lamproitic melts are generated by melting of metasomatized mantle enriched in lithophile and volatile elements of lithospheric mantle with peculiar evolution in each definite case (Gupta, 2015). New trace element data on minerals of the Gaussberg lamproites allowed us to obtain additional information on the geochemical specifics of lamproitic magmas and to estimate the nature of their source.

The study of trace components in liquidus olivines can be used to decipher their generation from peridotite or pyroxene mantle (Sobolev et al., 2007). In particular, the elevated Ni contents reaching 4900 ppm in the Gaussberg liquidus olivines (Fig. 9) could indicate the presence of olivine-free (pyroxenite) components in a mantle source (Sobolev et al., 2007). Olivines with high 100*Mn/Fe and the lowest Ni/(Mg/Fe)/1000 are in equilibrium with peridotite mantle, while olivines from melts generated from pyroxenite (olivine-free) source have the highest Ni/(Mg/Fe)/1000 and the lowest 100 Mn/Fe ratios (Fig. 14). The calculation of characteristic parameter X_{PX} using proposed (Sobolev et al., 2007) formula ($X_{PX}Ni = 10.54NiO/(MgO/FeO) − 0.4368$) for olivine phenocrysts in the Gaussberg lamproites suggests the contribution from 30 to 60% (on average, 50%) of pyroxenite matter in a melting source ($X_{PX}Ni \approx 0.5$) (Fig. 15).

Numerical modeling showed that recycled crustal material, if occurs in ascending plume, will melt at a depth of 150−170 km, thus forming andesitic melts, which are interacted with peridotite protolith to form reaction pyroxenite (Sobolev et al., 2005). During further ascent, reaction pyroxenite melts at a depth of 150 km with formation of high-Mg ferropicrites. At a depth of 100 km, mantle peridotite is involved in melting. The pyroxenite component in a source could be

formed both by assimilation of diverse crustal rocks and delamination of root parts of the lithosphere under plume impact (Sobolev et al., 2007). At the same time, the enriched source could be also obtained through metasomatic reworking of peridotite with formation of clinopyroxene and phlogopite (e.g., Grégoire et al., 2002), thus leading to the crystallization of olivines with elevated Ni concentrations and lowered Mn content relative to Fe.

Different assumptions were made on the origin of sources of ultra-potassic magmas. The study of lamproites from the Xiaogulihe Province led Sun et al. (2014) to conclude that these magmas were derived from the lower crustal phlogopite-bearing garnet source. This is consistent with experimental studies showing that lamproite (olivine−leucite) magmas could be derivatives of high-K olivine−pyroxenite melts, which were formed through the partial melting of phlogopite-bearing harzburgites or lherzolites under reduced conditions in the presence of hydrous fluid (Gupta, 1972; Foley, 1989, 1993; Foley et al., 2022). Primary melts derived from garnet pyroxenites, unlike peridotites, should be enriched in Al_2O_3 and significantly depleted in CaO (Zou et al., 2003). However, the Gaussberg liquidus olivines are relatively enriched in Ni, CaO, but are depleted in Al_2O_3, which can be explained by the heterogeneity of pyroxenite sources (Elkins et al., 2019; Sobolev et al., 2007). Compared to olivines from the Quaternary Xiaogulihe complex, the olivines of Gaussberg have sufficiently low Fe/Mn ratio (on average, ~ 62), which suggests more oxidized conditions of their generation (Herzberg, 2011; Kelley and Cottrell, 2009).

New experimental data show that important components of mantle source for the formation of ultra-potassic rocks are hydrous pyroxenites, which contain phlogopite or K-richterite (Foley et al., 2022). Thereby, initial magmas moving upwards could dissolve host peridotite rocks, which leads to the obliteration of "pyroxenite signature". In addition, the eruption of alkaline lavas of different composition on the adjacent territories also could be caused by the local heterogeneity of mantle source (Chayka et al., 2020).

Unlike the high-Mg alkaline basalts of the Jetty province, which are enriched in volatiles and, first of all, in CO_2 (reaching up to 8 wt % (Sushchevskaya et al., 2017)) and were formed by deep melting of volatile-rich metasomatized mantle, the Gaussberg melts are less enriched in volatiles. The quench glasses and melt inclusions in the phenocrysts of the Gaussberg lamproites contain CO_2 and H_2O-bearing fluids and other volatiles (S, Cl, P, F) (Savioli-Marziani, 2004; our data), but their concentrations indicate that the melt was undersaturated in volatile components. It is possible that the volatiles were inherited from primary melts derived from hydrous mantle source, for instance, from the phlogopite- and K amphibole-bearing pyroxenite. In addition, the Gaussberg melts
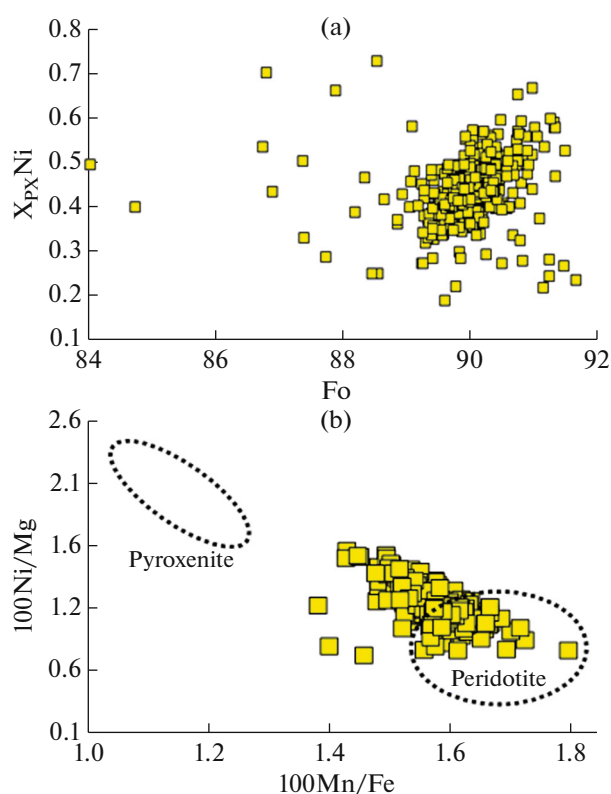
Fig. 15. Genetic role of olivine compositions. (a) Assessment of fraction of pyroxenite component in a melting source of Gaussberg. Calculation of characteristic parameter X_{PX} was carried out using formula $X_{PX}Ni = 10.54NiO/(MgO/FeO) − 0.4368$ (Sobolev et al., 2007). (b) compositional variations of olivines in the diagram $100Mn/Fe − 100Ni/Mg$ (Sobolev et al., 2007), which allows identification of pyroxenite and peridotite sources for primary melts (shown by fields).

were initially enriched in U and Th, so-called continental signatures, which indicate the contribution of fragments of continental lithosphere in melting (Sushchevskaya et al., 2014).

Based on isotope-geochemical studies, Sushchevskaya et al. (2017) proposed a model for the formation of mantle source of the studied lamproites of Gaussberg volcano from ancient material corresponding to the 2.2−2.4-Ga Paleoproterozoic lower crustal−upper mantle protolith mmixed with modern plume material (Sushchevskaya et al., 2017). Conditions for such mixing and melting could occur during ascent and propagation of Kerguelen plume in the vicinity or within the existing Antarctic−Indian spreading zone (Frey et al., 2000).

Thereby, according to the thermochemical model proposed by (Sobolev et al., 2009), conditions required for deep melting of metasomatized mantle could occur in the apical part of the plume beneath the continental margin. Its subsequent melting could lead to the appearance of low-degree enriched melts, some of which reached the surface, while others were retained and frozen in a mantle framework. This stage

was responsible for the appearance of alkaline magmatism in East Antarctica and southeastern India (Sushchevskaya et al., 2017). The local though attenuated thermal impact of the Kerguelen plume continues up to the present, which is indicated by the formation of the Ross and Herd volcanic islands within the Kerguelen plateau (Sushchevskaya et al., 2014). The subsequent plume-induced melting of ancient lithosphere domains of the Antarctic margin, which included the fragments of ultramafic rocks, pyroxenites, and veins or dikes of enriched alkaline basalts formed at different stages of the Gondwana evolution, led to the formation of lamproitic melts ejected by Gaussberg volcano. The peculiar isotopic characteristics of these low-degree melts correspond to enriched ancient continental mantle (Sushchevskaya et al., 2017).

Thus, the geochemical studies supplemented by data on olivine composition suggest that the formation of ultra-alkaline magmas in the Gaussberg volcano area could be related to melting of ancient continental lithosphere of Gondwana, which was heterogeneous and contained both peridotite mantle and fragments of hydrous pyroxenites.

CONCLUSIONS

Based on numerous new data (hundreds of analyses) obtained using high-precision modern analytical techniques, compositional variations of olivine, clinopyroxene, and leucite phenocrysts, as well as of spinel inclusions in olivine and quench glasses from lamproites of Gaussberg volcano (East Antarctica) were established. It was demonstrated that the majority of olivine phenocrysts are represented by sufficiently high-Mg compositions (Fo $_{89-91}$) with elevated Ni content (up to 4900 ppm). The study of a large data set of clinopyroxenes revealed two groups of coexisting clinopyroxenes, which differ in the Fe, Ti, Al, Cr, and Na contents and proportions of lithophile elements and are not related by a common differentiation trend. The first group characterizes the compositions of typical clinopyroxene phenocrysts that crystallized from the Gaussberg lamproitic magma. The second group (with elevated contents of FeO, Al_2O_3, and Na_2O and decreased contents of TiO_2, Cr_2O_3, NiO), which in previous works was termed "salite" or "green cores" (Foley, 1985; Foley and Jenner, 2004), has crystallized from different primary melts under distinct physical and chemical conditions. The compositions of typical leucite phenocrysts form a field with Fe_2O_3 content within 0.7–1.2 wt %. However, some resorbed leucite grains have the decreased iron contents (<0.45 wt % Fe_2O_3) and likely crystallized at more reduced conditions. The higher-Fe leucite varieties (up to 2.5 wt % Fe_2O_3) are typical of microlites or thin rims around phenocrysts.

The study of natural samples, existing experimental data, and numerical models allowed us to decipher the order and conditions of crystallization of the Gaussberg lamproites. Crystallization occurred in the following order: chromian spinel → chromian spinel + olivine → olivine + leucite (±chromian spinel) → olivine + leucite + clinopyroxene (±chromian spinel). Near-liquidus assemblage represented by phenocrysts of high-Mg olivine with inclusions of chromian spinel was formed within a temperature range from 1180 to 1250°C. Further crystallization of the melt with formation of olivine + leucite + clinopyroxene assemblage could occur at pressure below 2 GPa within the temperature range of 1070–1180°C, which corresponds to the water presence in the magmatic system. The redox conditions of lamproite crystallization estimated using different oxybarometers show wide variations from QFM−0.5 to QFM + 2.3, which highlights the need for additional studies and calibration of oxybarometer equations for ultra-alkaline system.

Using modern geochemical approaches based on the study of major and trace elements as well as their ratios in liquidus olivines, the type of primary source of Gaussberg magmas was determined. In addition to peridotite matter, melting involved rocks with signatures of pyroxenite mantle. Such rocks could be heterogeneous ancient lithosphere of Gondwana of peridotite and pyroxenite composition, which was involved in melting under the influence of Kerguelen plume.

The detailed mineralogical and geochemical studies of the Gaussberg lamproites showed that more reliable reconstruction of conditions of evolution and crystallization of such magmas requires additional experimental studies of phase equilibria and trace element partitioning between melt and crystalline phases in the ultra-potassic systems where "olivine + clinopyroxene + leucite" mineral association is stable. An open question is a source of clinopyroxene "green cores" with elevated FeO and Al_2O_3 contents in the Gaussberg lamproites and volcanic rocks from worldwide alkaline provinces. To solve this question, it is necessary to carry out additional detailed geochemical studies of phenocrysts from lavas and crystalline nodules in them.

CONFLICT OF INTEREST

The authors declare that they have no conflicts of interest.

OPEN ACCESS

SUPPLEMENTARY INFORMATION

REFERENCES

W. J. Atkinson, F. E. Hughes, and C. B. Smith, "A review of the kimberlitic rocks of Western Australia," In: *Kimberlites I: Kimberlites and Related Rocks,* Ed. by O. Kornprobst (Elsevier, Amsterdam, 1984), pp. 195–224.

R. Avanzinelli, T. Elliott, S. Tommasini, and S. Conticelli, "Constraints on the genesis of potassium-rich Italian volcanic rocks from U/Th disequilibrium," J. Petrol. **49**, 195–223 (2008).

C. G. Ballhaus, R. F. Berry, and D. H. Green, "High pressure experimental calibration of the olivine-orthopyroxene-spinel oxygen geobarometer: implications for the oxidation state of the upper mantle," Contrib. Mineral. Petrol. **107**, 27–40 (1991).

M. Barton and M. J. Van Bergen, "Green clinopyroxene and associated phases in a potassium-rich lava from Leucite Hills, Wyoming," Contrib. Min. Petrol. **77**, 101–114 (1981).

M. Barton, K. C. Varekamp, and M. J. van Bergen, "Complex zoing of clinopyroxenes in the lavas of Vulsini, Latium, Italy: evidence for magma mixing," J. Volcanol. Geotherm. Res. **14**, 361–388 (1982).

V. G. Batanova, I. A. Belousov, G. N. Savelieva, and A. V. Sobolev, "Consequences of chanellized and diffuse melt transport in supra-subduction zone mantle: Evidence from the Voykar ophiolite (Polar Ural)," J. Petrol. **52** (12), 2483–2521 (2011).

V. Batanova, A. V. Sobolev, and D. V. Kuzmin, "Trace element analysis of olivine: High precision analytical method for JEOL JXA-8230 electron probe microanalyser," Chem. Geol. **419**, 149–157 (2015).

D. Canil and Y. Fedortchouk, "Olivine–liquid partitioning of vanadium and other trace elements, with applications to modern and ancient picrites," Can. Mineral. **39**, 319–330 (2001).

S. Carbonin, G. Salviulo, R. Munno, and M. Desiderio, "Crystal–chemical examination of natural diopsides: some geometrical indications of Si–Ti tetrahedral substitution," Mineral. Petrol. **41**, 1–10 (1989).

I. F. Chayka, A. V. Sobolev, E. Izokh A.E. Andrey, V. G. Batanova, S. P. Krasheninnikov, CM. V. hervyakovskaya, A. Kontonikas-Charos, A. V. Kutyrev, B. M. Lobastov, and V. S. Chervyakovskiy, "Fingerprints of kamafugite-like magmas in Mesozoic lamproites of the Aldan Shield: evidence from olivine and olivine−hosted inclusions," Minerals **10** (4), 337 (2020). https://doi.org/10.3390/min10040337 www.mdpi (2020).com/journal/minerals

Y. Chen, Y. Zhang, D. Graham, S. Su, and J. Deng, "Geochemistry of Cenozoic basalts and mantle xenoliths in Northeast China," Lithos **96**, 108−126 (2007).

S. H. Choi, S. B. Mukasa, S. T. Kwon, and A. V. Andronikov, "Sr, Nd, Pb and Hf isotopic compositions of late Cenozoic alkali basalts in South Korea: evidence for mixing between the two dominant asthenospheric mantle domains beneath East Asia," Chem. Geol. **232**, 134−151 (2006).

Z. Y. Chu, J. Harvey, C. Z. Liu, J. H. Guo, F. Y. Wu, W. Tian, Y. L. Zhang, and Y. H. Yang, "Source of highly potassic basalts in northeast China: evidence from Re−Os, Sr−Nd−Hf isotopes and PGE geochemistry," Chem. Geol. **357**, 52−66 (2013).

K. D. Collerson and M. T. McCulloch, "Nd and Sr isotope geochemistry of leucite-bearing lavas from Gaussberg, East Antarctica," *Antarctic Earth Science*, Ed. by R. L. Oliver, P. R. James, and J. B. Jago, (Cambridge University Press, Cambridge, 1983), pp. 676−680.

L. A. Coogan, A. D. Saunders, and R. N. Wilson, "Aluminium-in-olivine thermometry of primitive basalts: Evidence of an anomalously hot mantle source for large igneous provences," Chem. Geol. **368**, 1−10 (2014).

G. R. Davies, A. J. Stolz, I. L. Mahotkin, G. M. Nowell, and D. G. Pearson, "Trace element and Sr−Pb−Nd−Hf isotope evidence for ancient, fluid-dominated enrichment of the source of Aldan shield lamproites," J. Petrol. **47**, 1119−1146 (2006).

L. L. Davis and D. Smith, "Ni-rich olivine in minettes from two Buttes, Colorado: a connection between potassic melts from the mantle and low Ni partition coefficients," Geochim. Cosmochim. Acta. **57** (1), 123−129 (1993).

J. M. Duke, "Distribution of the period four transition elements among olivine, calcic clinopyroxene and mafic silicate liquid: experimental results," J. Petrol. **17** (4), 499−521 (1976).

A. D. Edgar and R. H. Mitchell, "Ultra high pressure−temperature melting experiments on an SiO_2-rich lamproite from Smoky Butte, Montana: Derivation of siliceous lamproite magmas from enriched sources deep in the continental mantle," J. Petrol. **38** (6), 457−477 (1997).

M. Elburg and J. Foden, "Sources for magmatism in central Sulawesi: geochemical and Sr−Nd−Pb isotopic constraints," Chem. Geol. **156**, 67−93 (1999).

L. J. Elkins, B. Bourdon, and S. Lambart, "Testing pyroxenite versus peridotite sources for marine basalts using U-series isotopes," Lithos **332−333**, 226−244 (2019).

A. J. G. Ellison and P. C. Hess, "Raman-study of potassium-silicate glasses containing Rb+, Sr2+, Y3+ and Zr4+-implications for cation solution mechanisms in

multicomponent liquids," Geochim. Cosmochim. Acta. **58**, 1877−1887 (1994).

D. W. Fasshauer, B. Wunder, N. D. Chatterjee, and G. W. H. Hohne, "Heat capacity of wadeite-type K_2SiO_9 and the pressure-induced stable decomposition of K-feldspar," Contrib. Mineral. Petrol. **131**, 210−218 (1998).

S. F. Foley, "The oxidation state of lamproitic magmas," Min. Petr. Mitt. **34**, 217−238 (1985).

S. F. Foley, "Experimental constraints on petrology and Chemistry in lamproites: 1. The effect of water activity and oxygen fugacity," Eur. J. Mineral. **1**, 411−426 (1989).

S. F. Foley, "An experimental study of olivine lamproite: First results from the diamond stability field," Geochim. Cosmochim. Acta **57**, 483−489 (1993).

S. F. Foley and G. A. Jenner, "Trace element partitioning in lamproitic magmas—the Gaussberg olivine leucitite," Lithos **75**, 19−38 (2004).

S. F. Foley, G. Venturelli, D. H. Green, and L. Toscani, "The ultrapotassic Rocks: Characteristics, classification, and constraints for petrogenetic models," Earth Sci. Rev. **24**, 81−134 (1987).

S. F. Foley, D. E. Jacob, and H. St. C. O'Neil, "Trace element variations in olivine phenocrysts from Ugandan potassic rocks as clues to the chemical characteristics of parental magmas," Contrib. Mineral. Petrol. **162**, 1−20 (2011).

S. F. Foley, D. Prelevic, T. Rehfeldt, and D. E. Jacob, "Minor and trace elements in olivines as probes into early igneous and mantle melting processes," Earth. Planet. Sci. Lett. **363**, 181−191 (2013).

S. F. Foley, I. S. Ezad, S. R. van der Laan, and M. Pertermann, "Melting of hydrous pyroxenites with alkali amphiboles in the continental mantle: 1. Melting relations and major element compositions of melts," Geosci. Front. **13** (4), 101380 (2022).

C. E. Ford, D. G. Russel, J. A. Graven, and M. R. Fisk, "Olivine-liquid equilibria: temperature, pressure and composition dependence of the crystal/liquid cation partition coefficients for Mg, Fe^{2+}, Ca and Mn," J. Petrol. **24**, 256−265 (1983).

F. A. Frey, M. F. Coffin, and P. J. Wallace, "Origin and evolution of a submarine large igneous province: the Kerguelen Plateau and Broken Ridge, southern Indian Ocean," Earth Planet. Sci. Lett. **176**, 73−89 (2000).

X. Geng, Z. Liang, W. Zhang, Y. Liu, Z. Hu, and L. Deng, "Formation of green-core clinopyroxene in continental basalts through magmatic differentiation and crustal assimilation: Insights from in−situ trace element and Pb isotopic compositions," Lithos **410−411**, 106587 (2022).
https://doi.org/10.1016/j.lithos.2021.106587

Yu. S. Glebovsky, "Subice Brown-Gaussberg Ridge," Byull. Soviet Antarct. Expedition. **10**, 13−17 (1959).

D. A. Golynsky and Golynsky A. V. "Gaussberg rift—illusion or reality?" in *10th ISAES,* Ed. by A. K. Cooper, C. R. Raymond, et al., *U.S. Geol. Surv. Nat. Acad.; USGS OF-2007-1047, Extended Abstract 168.*

G. H. Grantham, "Weddell Sea tectonics and Gondwana break-up," Geol. Soc. London Spec. Publ. **108**, 63−71 (1996).

M. Gregoire, D. R. Bell, and A. P. Le Roex, "Trace element geochemistry of phlogopite-rich mafic mantle xenoliths:their classification and their relationship to phlogopite-bearing peridotites and kimberlites revisited," Contrib. Mineral. Petrol. **142**, 603−625 (2002).

A. K. Gupta, "The system forsterite−diopside−akermanite−leucite and its significance in the origin of potassium-rich mafic and ultramafic rocks," Am. Mineral. **57**, 1242−1259 (1972).

A. K. Gupta, *Origin of Potassium-Rich Silica-Deficient Igneous Rocks* (Springer, 2015),
https://doi.org/10.1007/978-81-322-2083−1_
http://www.springer.com/series/101721

A. K. Gupta and K. Yagi, *Petrology and Genesis of the Leucite−Bearing Rocks* (Springer, Berlin, 1980).

A. A. Gurenko, A. V. Sobolev, and N. N. Kononkova, "New petrologic data on ugandites from the East African rift, as revealed by study of magmatic inclusions in minerals," Dokl. Akad. Nauk SSSR **305**, 130−134 (1989).

S. R. Hart, J. Blusztajn, W. E. Lemasurier, and D. C. Rex, "Hobbs Coast Cenozoic volcanism: Inplications for the West Antarctic rift system," Chem. Geol. **139**, 223−248 (1997).

C. M.B. Henderson and D. Taylor, "An experimental study of the leucite mineral group," Progr. Exp. Petrol. **1**, 45−50 (1969).

C. Herzberg, "Basalts as temperature probes of Earth's mantle," Geology **39**, 1179−1180 (2011).

M. E. Jankovics, Z. Taracsák, G. Dobosi, A. Embey-Isztin, A. Batki, S. Harangi, and C. A. Hauzenberger, "Clinopyroxene with diverse origins in alkaline basalts from the western Pannonian Basin: Implications from trace element characteristics," Lithos **262**, 120−134 (2016).

A. L. Jaques, J. D. Lewis, and C. B. Smith, "The kimberlites and lamproites of Western Australia," Geol. Surv. West. Aust. Bull. **132**, 269 (1986).

A. L. Jaques, J. D. Lewis, C. B. Smith, G. P. Gregory, J. Ferguson, B. W. Chappell, and M. T. McCulloch, "The diamond-bearing ultrapotassic (lamproitic) rocks of the West Kimberly region, Western Australia," In: *Kimberlites I: Kimberlites and Related Rocks,* Ed. by J. Kornprobst,(Elsevier, Amsterdam, 1984), pp. 225−254.

E. J. Jarosewich, J. A. Nelen, and J. A. Norberg, "Reference samples for electron microprobe analysis," Geostand. Newslett. **4**, 43−47 (1980).

K. A. Kelley and E. Cottrell, "Water and the oxidation state of subduction zone magmas," Science **325**, 605−607 (2009).

T. Kiritani, J. I. Kimura, E. Ohtani, H. Miyamoto, and K. Fukuyama, "Transition zone origin of potassic basalts from Wudalianchi volcano, northeast China," Lithos **156−159**, 1−12 (2013).

S. C. Kohn and P. F. Schofield, "The importance of melt composition in controlling trace-element behavior: an experimental study of Mn and Zn partitioning between forsterite and silicate melts," Chem. Geol. **117**, 73−87 (1994).

A. N Koshlyakova, A. V. Sobolev, S. P. Batanova V. G. Krasheninnikov, and A. A. Borisov, "Ni parti-

tioning between olivine and highly alkaline melts: An experimental study," Chem. Geol. **587**, 120615 (2022).

G. L. Leitchenkov and Yu. B. Guseva, "Structure and evolution of the Earth's crust of the sedimentary basin of the Davis Sea, East Antarctica," in *Scientific Results of Geological—Geophysical Studies in Antarctica,* Ed. by G. L. Leitchenkov and A. A. Laiba (VNIIOkeangeologiya, St. Petersburg, 2006), pp. 101−115.

J. Q. Liu, L. H. Chen, X. J. Wang, X. Y. Zhang, G. Zeng, S. Erdmann, D. T. Murphy, K. D. Kenneth, T. Komiya, and L. Krmíček, "Magnesium and zinc isotopic evidence for the involvement of recycled carbonates in the petrogenesis of Gaussberg lamproites, Antarctica," Chem. Geol. **609**, 121067 (2022).

G. Mallmann and H. St. G. O`Neill, "Calibration of an empirical thermometer and oxybarometer based on the partitioning of Sc, Y and V between olivine and silicate melt," J. Petrol. **54** (5), 933−949 (2013).

D. McKenzie, "Some remarks on the movement of small melt fractions in the mantle," Earth. Planet. Sci. Lett. **95**, 53−72 (1989).

N. A. Migdisova, N. M. Sushchevskaya, A. V. Luttinen, and E. M. Mikhal'skii, "Variations in the composition of clinopyroxene from the basalts of various geodynamic settings of the Antarctic region," Petrology **12** (2), 206−224 (2004).

M. S. Milman-Barris, J. R. Beckett, M. B. Baker, A. E. Hofmann, Z. Morgan, M. R. Crowley, D. Vielzeuf, and E. Stolper, "Zoning of phosphorus in igneous olivines," Contrib. Mineral. Petrol. **155**, 739−765 (2008).

R. H. Mitchell and S. C. Bergman, *Petrology of Lamproites* (Plenum, New York, 1991).

N. Morimoto, J. Fabries, A. K. Fergusson, I. V. Ginzburg, M. Ross, F. A. Seifert, J. Zussman, K. Aoki, and G. Gottardi, "Nomenclature of pyroxenes," Am. Mineral. **73**, 1123−1133 (1988).

S. A. Morse, "Alkali feldspar−water at 5 kb," Carnegie Inst Wash Yearb. **67**, 120−126 (1969).

D. T. Murphy, K. D. Collerson, and B. S. Kamber, "Lamproites from Gaussberg, Antarctica: possible transition zone melts of Archaean subducted sediments," J. Petrol. **43** (6), 981−1001 (2002).

B. O. Mysen and P. Richet, *Silicate Glasses and Melts* (Elsevier, 2018).

B. O. Mysen and D. Virgo, "Trace element partitioning and melt structure: an experimental study at 1 atm. pressure," Geochim. Cosmochim. Acta **44** (12), 1917−1930 (1980).

K. Nag, M. Arima, and A. K. Gupta, "Experimental study of the join forsterite−diopside−leucite and forsterite−leucite−akermanite up to 2.3 GPa [P (H2O) = P (total)] and variable temperatures; its petrological significance," Lithos **98** (1−4), 177−194 (2007).

D. R. Nelson, M. T. McCulloch, and S. -S. Sun, "The origins of ultrapotassic rocks as inferred from Sr, Nd, and Pb isotopes," Geochim. Cosmochim. Acta **50**, 231−245 (1986).

G. S. Nikolaev, A. A. Ariskin, G. S. Barmina, M. A. Nazarova, and R. R. Almeev, "Test of the Ballhaus−Berry−Green Ol−Opx−Sp oxybarometer and calibration of a new equation for estimating the redox state of melts saturated with olivine and spinel," Geochem. Int. **54** (4), 301−320 (2016).

G. Pe-Piper, "Zoned pyroxenes from shoshonite lavas of Lesbos, Greece: inferences concerning shoshonite petrogenesis," J. Petrol. **25**, 453−472 (1984).

D. R. Peacor, "A high temperature single crystal diffractometer study of leucite (K, Na) $AlSi_2O_6$," Z. Kristallogr. **127**, 213−224 (1968).

PetDB: https://search.earthchem.org/

A. Poldervaart and H. H. Hess, "Pyroxenes in the crystallization of basaltic magma," J. Geol. **59** (5), 472−489 (1951).

D. Prelevic and S. F. Foley, "Accretion of arc-oceanic lithospheric mantle in the Mediterranean: evidence from extremely high-Mg olivines and Cr-rich spinel inclusions in lamproites," Earth Planet. Sci. Lett. **256**, 120−135 (2007).

D. Prelevic, S. F. Foley, R. Romer, and S. Conticelli, "Mediterranean tertiary lamproites derived from multiple source components in postcollisional geodynamics," Geochim. Cosmochim. Acta. **72**, 2125−2156 (2008).

D. Prelevic, D. E. Jacob, and S. F. Foley, "Recycled continental crust is an essential ingredient of Mediterranean orogenic mantle lithosphere," Earth Planet. Sci. Lett. **362**, 187−197 (2013).

E. Salvioli-Mariani, L. Toscani, and D. Bersani, "Magmatic evolution of the Gaussberg lamproite (Antarctica): volatile content and glass composition," Mineral. Mag. **68**, 83−100 (2004).
https://doi.org/10.1180/0026461046810173

J. W. Sheraton, "Chemical analyses of rocks from East Antarctica," Bur. Min. Res. Record. **1981/14**, 67−68 (1981).

J. W. Sheraton, "Chemical analyses of rocks from East Antarctica: Part 2. Bur. Min. Res. Record. **1985/12,** (1985).

J. W. Sheraton and A. Cundari, "Leucitites from Gaussberg, Antarctica," Contrib. Mineral. Petrol. **71**, 417−427 (1980).
https://doi.org/10.1007/BF00374713

T. A. Shishkina, M. V. Portnyagin, R. E. Botcharnikov, R. R. Almeev, A. V. Simonyan, D. Garbe-Schönberg, S. Schuth, M. Oeser, and F. Holtz, "Experimental calibration and implications of olivine-melt vanadium oxybarometry for hydrous basaltic arc magmas," Am. Mineral. **103**, 369−383 (2018).

T. A. Shishkina, M. O. Anosova, N. A. Migdisova, M. V. Portnyagin, N. M. Sushchevskaya, and V. G. Batanova, "Trace elements in olivine of volcanic rocks: application to the study of magmatic systems," Geochem. Int. **61** (1), 1−23 (2023).

H. Sigurdsson, "Spinels in leg 37 basalts and peridotites: phase chemistry and zoning," Proc. Deep Sea Drilling Project, Initial Rept. **37**, 883−891 (1977).

J. L. Smellie and K. D. Collerson, "Gaussberg: volcanology and petrology," Geol. Soc. London, Mem. **55**(1), 615-628 (2021).
https://doi.org/10.1144/M55-2018−85

A. V. Sobolev, N. V. Sobolev, S. B. Smith, and N. N. Kononkova, "New data on the petrology of the olivine lamproites of Western Australia revealed by the study of magmatic

inclusions in olivine," Dokl. Akad. Nauk SSSR **284** (1), 196−201 (1976).

A. V. Sobolev, A. W. Hofmann, S. V. Sobolev, and I. K. Nikogosian, "An olivine-free mantle source of Hawaiian shield basalts," Nature **434**, 590−597 (2005). https://doi.org/10.1038/nature03411

A. V. Sobolev, A. W. Hofmann, D. V. Kuzmin, G. M. Yaxley, N. T. Arndt, S. L. Chung, L. V. Danyushevsky, T. Elliott, F. A. Frey, M. O. Garcia, A. A. Gurenko, V. S. Kamenetsky, A. C. Kerr, N. A. Krivolutskaya, V. V. Matvienkov, I. K. Nokogosian, A. Rocholl, I. A. Sigurdsson, N. M. Suschevskaya, and M. Teklay, "The amount of recycled crust in sources of mantle-derived melts," Science **316** (5823), 412−417 (2007).

A. V. Sobolev, S. V. Sobolev, D. V. Kuzmin, K. N. Malich, and A. G. Petrunin, "Siberian meimechites: origin and relation to flood basalts and kimberlites," Russ. Geol. Geophys. **50** (12), 1293−1334 (2009).

A. V. Sobolev, E. V. Asafov, A. A. Gurenko, N. T. Arndt, V. G. Batanova, M. V. Portnyagin, D. Garbe-Schonberg, and S. P. Krasheninnikov, "Komatiites reveal a hydrous Archaean deep-mantle reservoir," Nature **531**, 628−632 (2016).

S.-S. Sun and W. F. McDonough, "Chemical and isotopic systematics of oceanic basalts: implications for mantle composition and processes," *Magmatism in the Ocean Basins*, Ed. by A. D. Suanders and M. J. Norry, Geol. Soc. Spec. Publ. **42**, 313−345 (1989).

Y. Sun, J. Ying, X. Zhou, J. Shao, Z. Chu, and B. Su, "Geochemistry of ultrapotassic volcanic rocks in Xiaogulihe NE China: Implications for the role of ancient subducted sediments," Lithos **208−209**, 53−66 (2014).

N. M. Sushchevskaya, N. A. Migdisova, A. V. Antonov, R. Sh. Krymsky, B. V. Belyatsky, D. V. Kuzmin, and Ya. V. Bychkova, "Geochemical features of the Quaternary lamproitic lavas of Gaussberg Volcano, East Antarctica: result of the impact of the Kerguelen Plume," Geochem. Int. **52** (12), 1030−1048 (2014).

N. M. Sushchevskaya, B. V. Belyatsky, E. P. Dubinin, and O. V. Levchenko, "Evolution of the Kerguelen plume and its impact upon the continental and oceanic magmatism of East Antarctica," Geochem. Int. **55** (9), 775−791 (2017).

N. M. Sushchevskaya, B. V. Belyatsky, D. A. Tkacheva, G. L. Leitchenkov, D. V. Kuzmine, and A. V. Zhilkina, "Early Cretaceous alkaline magmatism of East Antarctica: peculiarities, conditions of formation, and relationship with the Kerguelen Plume," Geochem. Int. **56** (11), 1051−1070 (2018).

R. N. Thompson, "Primary basalts and magma genesis (III), Alban hills, Roman Comagamatic Province, central Italy," Contrib. Mineral. Petrol. **60**, 91−108 (1977).

R. J. Tingey, I. McDougall, and A. J. W. Gleadow, "The age and mode of formation of Gaussberg, Antarctica," J. Geol. Soc. Austral. **30**, 241−246 (1983).

M. J. Toplis, "The thermodynamics of iron and magnesium partitioning between olivine and liquid: criteria for assessing and predicting equilibrium in natural and experimental systems," Contrib. Mineral. Petrol. **149**, 22−39 (2005).

O. F. Tuttle and N. L. Bowen, "Origin of granite in the light of experimental studies in the system $NaAlSi_3O_8$−$KAlSi_3O_8$−SiO_2−H_2O," Geol. Soc. Am. Mem. *74*, 153 (1958).

E. von Drygalski, *The Southern Ice−Continent: The German South Polar Expedition Aboard the Gauss, 1901−1903* (Bluntisham Books−Erskine Press, Harleston, 1989).

O. S. Vyalov and V. S. Sobolev, "Gaussberg, Antarctica, Int. Geol. Rev. **1** (7), 30−40 (1959).

C. Wagner and D. Velde, "The mineralogy of K-richterite-bearing lamproites," Am. Mineral. **71**, 17−37 (1986).

R. W. Williams, K. D. Collerson, J. B. Gill, and C. Deniel, "High Th/U ratios in subcontinental lithospheric mantle: mass spectrometric measurement of Th isotopes in Gaussberg lamproites," Earth Planet. Sci. Lett. **111**, 257−268 (1992).

M. Zhang, P. Suddaby, R. N. Thompson, M. F. Thirlwall, and M. A. Menzies, "Potassic volcanic rocks in NE China: geochemical constraints on mantle source and magma genesis," J. Petrol. **36**, 1275−1303 (1995).

M. Zhang, P. Suddaby, S. Y. O'Reilly, M. Norman, and J. X. Qiu, "Nature of the lithospheric mantle beneath the eastern part of the Central Asian fold belt: mantle xenoliths evidence," Tectonophysics **328**, 131−156 (2000).

H. Zou, M. R. Reid, Y. Liu, Y. Yao, X. Xu, and Q. Fan, "Constraints on the origin of historic potassic basalts from northeast China by U−Th disequilibrium data," Chem. Geol. **200**, 189−201 (2003).

Translated by M. Bogina